RSC Advances

REVIEW

View Article Online
View Journal | View Issue

Cite this: *RSC Adv.*, 2026, **16**, 23295

Photocatalytic CO_2 reduction to methanol: from mechanistic insights to reactor design integration

Cheng Zuo, Jing Wang, Chunling Xin* and Qian Su*

The conversion of CO_2 into high-value fuels, particularly methanol, represents a promising pathway for closing the carbon cycle and storing intermittent solar energy. While significant progress has been made in photocatalyst development, the transition from laboratory scale to industrial application remains hindered by low quantum efficiency and mass transfer limitations. This review systematically examines the state-of-the-art in photocatalytic CO_2 reduction, with a specific focus on methanol production. Unlike previous reviews that isolate catalyst materials from reactor engineering, this paper bridges the gap between intrinsic catalytic mechanisms and macroscopic reactor design. We first elucidate the reaction pathways favoring methanol selectivity over competing products such as CO and CH_4. Subsequently, we critically analyze optimization strategies for metal-based, metal-free, and MOF catalysts, emphasizing defect engineering and heterojunction construction. Crucially, the evolution of photoreactors is discussed in depth, highlighting the distinct mechanistic and mass-transfer challenges between liquid-phase and gas-phase reaction systems. Furthermore, we evaluate advanced engineering strategies, ranging from concentrated solar irradiation with precise thermal management to optofluidic microreactors, demonstrating how they overcome traditional photon flux limitations and multiphase mass transfer resistance. Finally, we propose a roadmap for future research, advocating for the integrated design of catalyst-reactor systems and the exploration of photo-thermal/electro-coupled technologies.

Received 27th February 2026
Accepted 4th April 2026

DOI: 10.1039/d6ra01735e

rsc.li/rsc-advances

1. Introduction

The relentless rise in atmospheric CO_2 concentrations has precipitated a global climate crisis, necessitating the urgent development of Carbon Capture, Utilization, and Storage (CCUS) technologies. Among these approaches, artificial photosynthesis, which refers to the photocatalytic reduction of CO_2, offers a compelling solution. It converts a greenhouse gas into energy-dense fuels using solar energy.[1–4]

While CO_2 reduction can yield various products including CO, methane, formic acid, and ethanol, methanol (CH_3OH) stands out as a premier target. As a liquid fuel under ambient conditions, methanol possesses a high volumetric energy density (15.6 MJ L^{-1}), is easily transportable, and serves as a versatile feedstock for the chemical industry.[5] However, producing methanol is kinetically and thermodynamically challenging compared to CO or HCOOH due to the involvement of six electrons and protons, making selectivity control a major hurdle.

Despite decades of research since the pioneering work of the researchers,[6,7] the overall efficiency of photocatalytic methanol production remains low. The bottleneck lies not only in the recombination of photogenerated carriers on the catalyst surface but also in the inefficient photon and mass transport within conventional reactors. This review aims to provide a holistic view, linking the microscopic design of catalysts with the macroscopic engineering of reactors, specifically highlighting emerging microreactor technologies that offer solutions to historical limitations.

2. Mechanistic fundamentals of CO_2 reduction to methanol

The photocatalytic conversion of CO_2 to methanol involves a complex multi-electron transfer process. The general photocatalytic steps, including light absorption, charge separation and surface reaction, are well understood. However, the specific pathway toward methanol formation still demands precise control.[8]

2.1. Thermodynamics and kinetics

The reduction potential for CO_2 to methanol is −0.38 V *vs.* NHE (at pH 7), which is thermodynamically feasible for many semiconductors (CB > −0.38 V). However, the reaction competes with the hydrogen evolution reaction (HER) and the formation of other C1 products.[9,10]

College of Chemistry & Chemical Engineering and Environmental Engineering, Weifang University, Weifang, 261061, China. E-mail: xinchunling@wfu.edu.cn; 20220033@wfu.edu.cn

$$CO_2 + 2H^+ + 2e^- \rightarrow CO + H_2O\ (-0.53\ V)$$

$$CO_2 + 8H^+ + 8e^- \rightarrow CH_4 + 2H_2O\ (-0.24\ V)$$

$$CO_2 + 6H^+ + 6e^- \rightarrow CH_3OH + H_2O\ (-0.38\ V)$$

As shown in Fig. 1, to selectively produce methanol, the catalyst must facilitate the stepwise hydrogenation of intermediates such as *CO → *CHO → *CH_2O → *CH_3O → CH_3OH, while suppressing the full deoxygenation to methane or the desorption of CO.[11–13]

2.2. Key challenges in photocatalytic CO_2 reduction to methanol

Despite the promise of photocatalytic technology, the efficient conversion of CO_2 to methanol is hindered by several fundamental physicochemical barriers. First and foremost is the challenge of CO_2 activation. As a linear, centrosymmetric molecule with a C=O bond energy of approximately 805 kJ mol^{-1}, CO_2 is chemically inert and thermodynamically stable. Consequently, the initial adsorption and subsequent bending of the linear CO_2 molecule on the photocatalyst surface are critical prerequisites for reducing the activation energy barrier. Without effective surface active sites to induce this structural distortion, the reductive attack by photogenerated electrons becomes kinetically sluggish.

Furthermore, selectivity control remains a formidable obstacle in the reaction pathway. The photoreduction of CO_2 involves multiple proton-coupled electron transfer steps, leading to a diverse range of C_1 and C_2+ products. Steering the reaction specifically toward methanol requires precise control over intermediate binding energies. Methanol formation is a 6-electron reduction process. A major difficulty lies in suppressing the competitive over-reduction to methane and the thermodynamically favorable hydrogen evolution reaction. Methane formation is an 8-electron process and both reactions often dominate on many semiconductor surfaces.

Finally, the issue of product desorption critically affects the overall yield and catalyst stability. Methanol molecules formed on the catalyst surface are prone to accumulation, which can block active sites or, more detrimentally, undergo reverse oxidation by photogenerated holes to form formaldehyde or revert to CO_2. Therefore, facilitating the timely desorption of methanol from the catalyst surface is essential to prevent product degradation and maintain continuous catalytic turnover. Addressing these interconnected challenges of activation, selectivity, and desorption requires a synergistic approach combining surface engineering with reactor design.

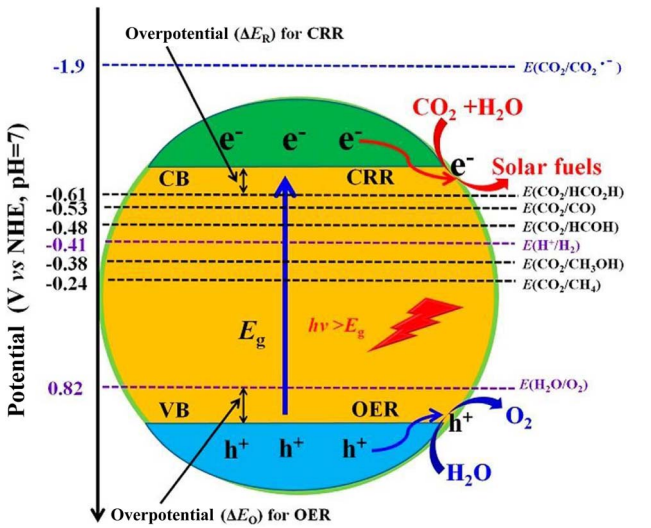

Fig. 1 Schematic of the photocatalytic reaction mechanism. Figure adapted from ref. 13 with permission from American Chemical Society, copyright 2019.

3. Photocatalyst materials and design strategies

3.1. Photocatalyst materials

Effective catalysts must possess adequate band gaps, high surface areas, and specific active sites for methanol synthesis.[14,15]

3.1.1. Metal-based catalysts

3.1.1.1. Metal oxides. Metal oxides represent one of the most extensively studied classes of photocatalysts for CO_2 reduction to methanol due to their abundance, low toxicity, and relatively high stability. Metal oxides are widely studied photocatalyst materials for CO_2 photocatalytic reduction. Some transition metal oxides containing metal cations (*e.g.*, Ti^{4+}, Zr^{4+}, Ta^{5+}, Nb^{5+}, Mo^{6+}, and W^{6+}), main-group metal oxides containing metal cations (*e.g.*, In^{3+}, Ga^{3+}, Sn^{4+}, Ge^{4+}, and Sb^{5+}), and lanthanide metal oxides containing metal cations (*e.g.*, La^{3+}, Ce^{4+}) were widely used in the field of photoreduction of CO_2.[16,17] Among them, Zinc Oxide (ZnO) and Copper Oxides (CuO/Cu_2O) have garnered significant attention.[18–20] However, single-component metal oxides often suffer from wide bandgaps restricting visible light absorption, rapid charge recombination, and limited surface active sites. Recent advancements have focused on overcoming these bottlenecks through strategic heterojunction construction, defect engineering, and morphology control to enhance methanol selectivity and yield.[21,22]

Copper is a common metallic element that is widely available and cheap. Copper oxide and cuprous oxide are widely used in the photocatalytic field and are mainly applied in the photocatalytic reduction of CO_2. Copper oxide or cuprous oxide, as well as most copper-based semiconductors, tend to reduce CO_2 to methanol. In the process of CO_2 reduction, when the hydrogen ions become hydrogen radicals, the electrons captured by Cu^{2+} are consumed, and Cu^+ is oxidized to produce Cu^{2+}. Specific reactions are shown in Fig. 2.[15] The reason for the better photocatalytic performance of copper-based semiconductors lies in the fact that the copper element inhibits the complexation of the photogenerated carriers when it undergoes the conversion in different valence states. However, the practical application of copper oxides including CuO and Cu_2O is

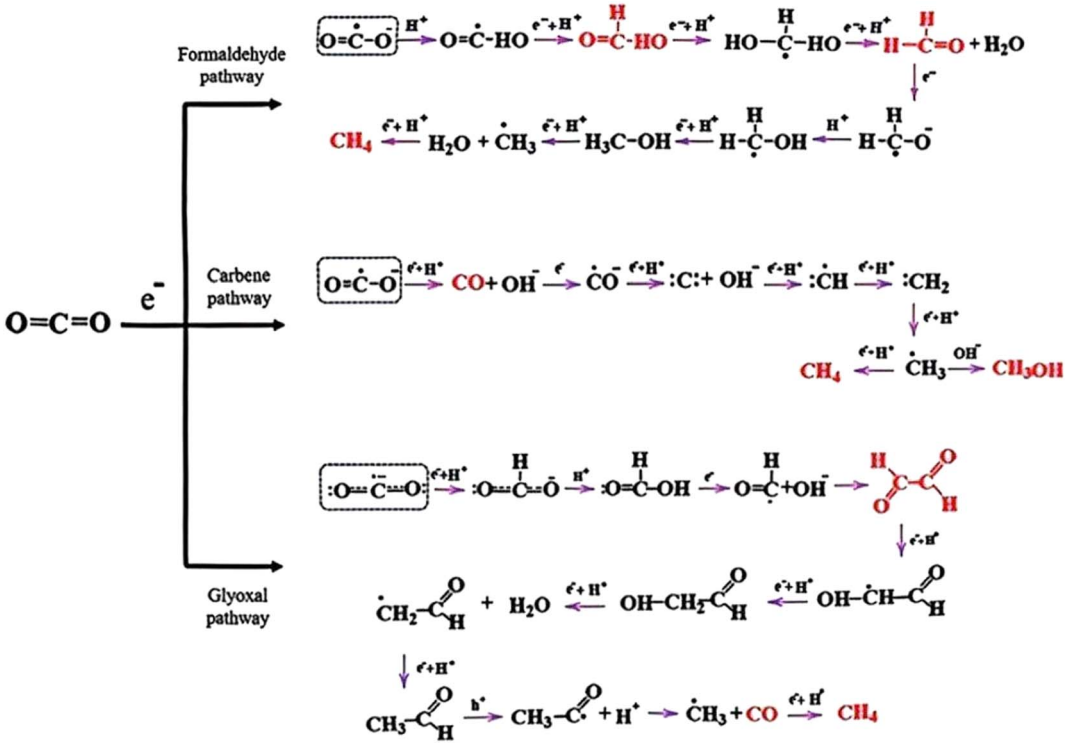

Fig. 2 Reaction pathway of photocatalytic reduction of CO_2 with Cu-based catalysts. Figure adapted from ref. 15 with permission from RSC, copyright 2022.

Table 1 Various performance optimization strategies for catalysts

Catalysts	Main product	Product rate	Ref.
C–TiO_2	HCOOH	2634 μmol g^{-1}	83
N–TiO_2	CH_3OH	20 μmol g^{-1}	84
Co–TiO_2	CH_3OH	6.5 μmol g^{-1}	85
Ag–TiO_2	CH_4	2.64 μmol g^{-1} h^{-1}	86
In–TiO_2	CH_4	1156 μmol g^{-1}	87
$FeTiO_3/TiO_2$	CH_3OH	0.46 μmol g^{-1} h^{-1}	88
CdS/TiO_2	CH_4	1.5 μmol g^{-1} h^{-1}	89

often hindered by severe photo-corrosion such as the self-reduction of Cu_2O and rapid charge recombination. To mitigate these stability-activity trade-offs, constructing Z-scheme heterojunctions has proven particularly effective, as it spatially separates charges and directs oxidative holes away from the unstable oxide lattice. For instance, Perini *et al.* constructed a TNT@PDA/Cu_2O/Au Z-scheme heterojunction, where TiO_2 nanotubes and Cu_2O were coupled with Au nanoparticles. This design facilitated a Z-scheme charge transfer mechanism that preserved the high reduction potential of electrons in Cu_2O while using Au as electron traps to suppress recombination, achieving a methanol Faraday efficiency of 47.4%.[23] Beyond electronic modulation, optimizing microscopic morphology to enhance mass transfer is equally critical. Gusain *et al.* fabricated rGO–CuO nanocomposites with varying CuO nanorod widths. They found that wider nanorods (10–15 nm) provided more active sites and, when combined with the conductive rGO network, significantly enhanced electron transport, resulting in a methanol yield of 1282 μmol g^{-1}.[24] Additionally, Movahed *et al.* developed a Fe_3O_4@N–C/Cu_2O core–shell nanostructure, demonstrating that the N–C shell not only improved visible light absorption but also protected the catalyst and facilitated charge separation, leading to a high methanol yield of 440 μmol g^{-1} with excellent cyclic stability.[25] These studies collectively suggest that for copper-based oxides, the design priority must shift from simple synthesis to engineering protective charge-transfer pathways like Z-schemes and robust microstructures.

ZnO, while abundant and non-toxic, typically suffers from a wide bandgap that restricts visible light utilization. Recent strategies have focused on sensitizing ZnO through doping or coupling with narrow-bandgap semiconductors to form functional heterojunctions. Al-Anazi *et al.* achieved a breakthrough methanol production rate of 156.04 μmol g^{-1} h^{-1} by synthesizing a porous Li_2MnO_3/ZnO S-scheme heterojunction. In this system, the synergy between the two semiconductors allowed for efficient spatial charge separation, where photo-electrons on the Li_2MnO_3 conduction band reduced CO_2 while holes on the ZnO valence band oxidized water.[26] Similarly, Getahun *et al.* utilized a 3D nanotube array (MeNTA) substrate to support amine-loaded CuO/ZnO, creating a system with a large specific surface area and intimate interfacial contact. This p–n heterojunction design, combined with the CO_2-capturing ability of amines, achieved a remarkable methanol yield of 4.5 mmol g^{-1}.[27] Furthermore, doping strategies, such as the formation of CuO/ZnO heterojunctions by Sahoo *et al.*, have been shown to

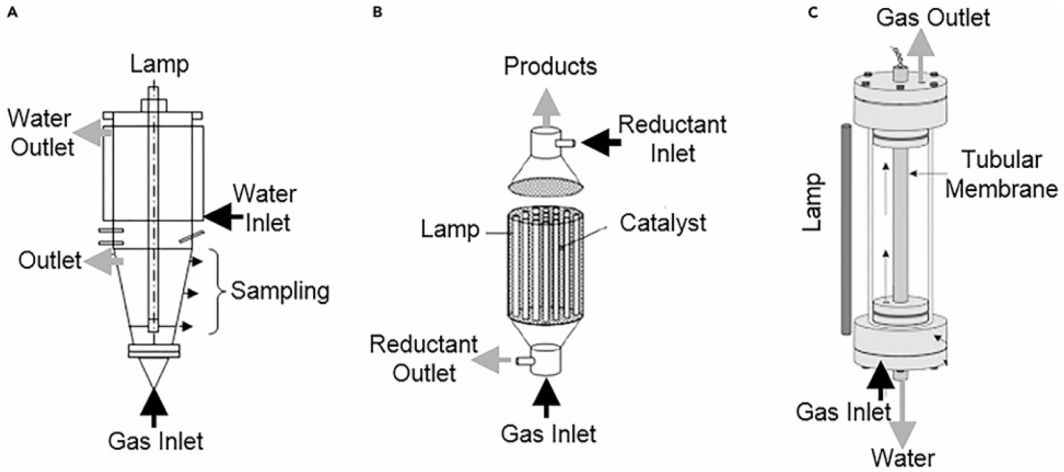

Fig. 3 Schematic representation of three typical photoreactor configurations: (A) slurry type, (B) fixed bed type, and (C) membrane photoreactor. Figure adapted from ref. 97 with permission from Elsevier, copyright 2023.

introduce oxygen vacancies and effectively extend the average electron lifetime. Their study confirmed that the coupling of CuO significantly improved charge separation efficiency (D value) compared to pure ZnO, resulting in a methanol yield of 26.85%.[28] While these modifications successfully address light absorption, the selectivity for methanol over CO or CH_4 remains a persistent challenge for ZnO-based materials.

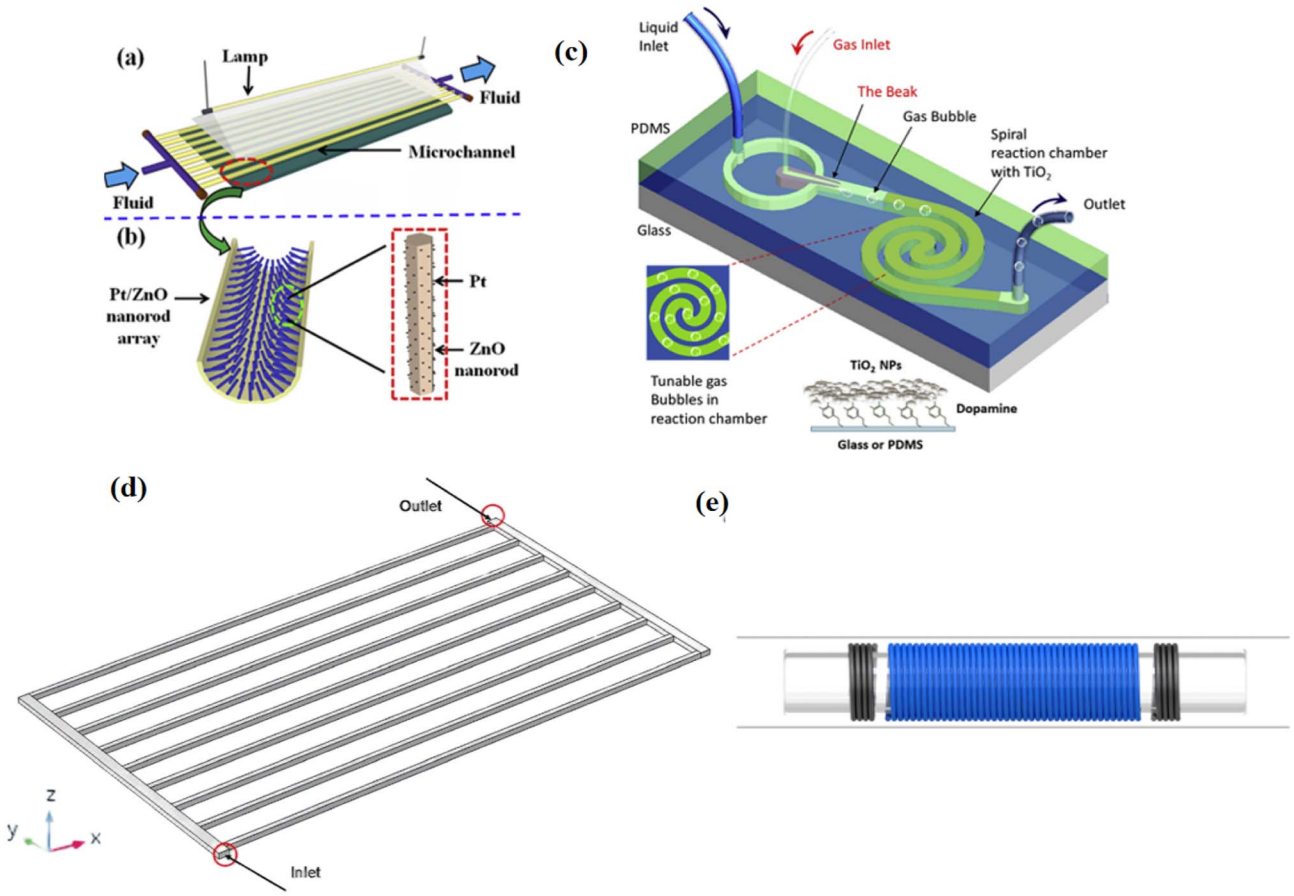

Fig. 4 Main types of microreactor structures used in the field of photo-(electro)catalysis: (a and b) multi-capillary, (c) single channel, (d) multiphase and (e) coil-type. Figure (a) and (b), (c), (d) reproduced from ref. 124, 125, 126 and 127 with permission from Elsevier, copyright 2023, 2020, 2026, 2017.

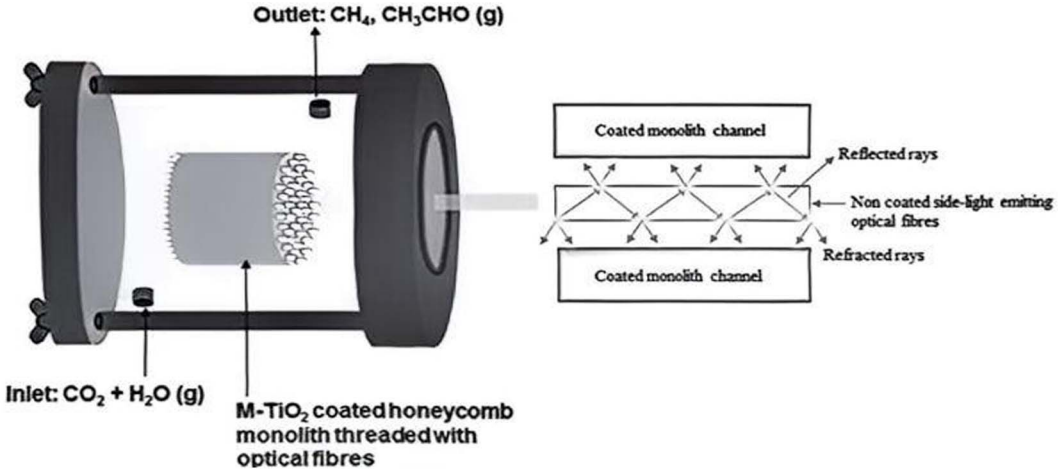

Fig. 5 The photocatalytic monolithic microreactor design integrating optical fibers for internal illumination.[128] Figure adapted from ref. 128 with permission from Elsevier, copyright 2016.

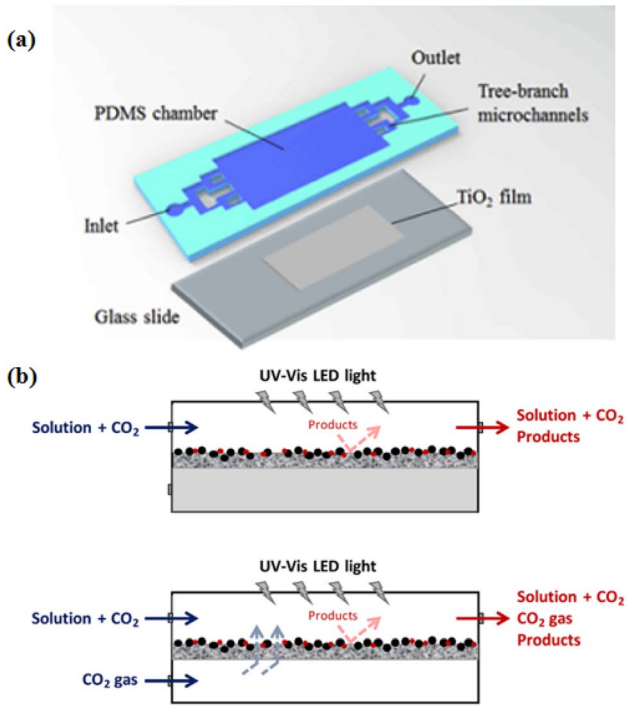

Fig. 6 Schematic diagram of the microreactor unit: (a) traditional single-layer membrane (b) double-layer transportation method for enhanced gas diffusion. Figure (a) and (b) reproduced from ref. 132 and 134 with permission from Elsevier, copyright 2017 and 2023.

From a mechanistic perspective, the key to unlocking high methanol selectivity in metal oxides lies in stabilizing the OCH_3 intermediate, which is often the rate-determining step. Future research should prioritize surface interface engineering, specifically creating oxygen vacancies or specific metal-defect sites to fine-tune intermediate binding energies. This strategy has been validated in CQD-modified Cu_2O as reported by Li *et al.*[29] Moreover, bridging the gap between laboratory powder synthesis and scalable application requires integrating these optimized metal oxide catalysts into continuous-flow microreactors. This integration would not only enhance mass transfer and product removal but also provide a controlled microenvironment to suppress competitive reactions like hydrogen evolution, thereby maximizing the practical potential of metal oxide photocatalysts.

3.1.1.2. Metal sulfides. Metal sulfides have emerged as a prominent class of photocatalysts for CO_2 reduction due to their suitable band positions, tunable electronic structures, and excellent visible-light responsiveness. Unlike metal oxides, the valence band of metal sulfides usually consists of S 3p orbitals, which are more negative than O 2p orbitals, resulting in a narrower bandgap that facilitates efficient utilization of the solar spectrum.[30] However, pristine metal sulfides often suffer from rapid charge recombination and photocorrosion. Recent research has focused on overcoming these limitations through structural engineering, elemental doping, and heterojunction construction to enhance methanol selectivity and yield.

ZnS based materials are widely studied due to their favorable conduction band potential for CO_2 reduction, though their wide bandgap limits visible light absorption.[31] To address this, doping strategies have proven effective. For instance, Mohamed *et al.* synthesized Pt-doped mesoporous ZnS, where Pt acts as an electron trap to inhibit charge recombination and the mesoporous structure provides abundant active sites.[32] The 1.5% Pt/ZnS achieved a methanol yield of 400 μmol g^{-1} in 9 hours, significantly outperforming pristine ZnS. Similarly, Imran *et al.* demonstrated that Indium-doped ZnS ($ZnIn_2S_4$) microspheres possess a narrowed bandgap (2.1 eV) and higher oxygen vacancy concentration compared to cubic ZnS (3.8 eV), leading to enhanced photocatalytic performance. Furthermore, modifying the lattice structure is also crucial.[31] Zhang *et al.* engineered copper-doped ZnS with internal sphalerite–wurtzite (S–W) phase junctions. The synergy between Cu doping and the S–W junction not only broadened light absorption but also enhanced the binding of *CO intermediates, although their work focused

Table 2 Comparison of typical reactor configurations for photocatalytic CO_2 reduction

Reactor type	Key features	Advantages	Limitations	Ref.
Twin reactor	Separated redox chambers connected by mediator	Suppresses reverse reaction; stoichiometric product generation	Complex system design; mediator stability	116
Monolith reactor	Honeycomb structure with thin catalyst coating	High throughput; excellent light utilization; high product yield	Mass transfer limited by diffusion in channels	129
Continuous flow microreactor	Microchannels with laminar flow	Precise residence time control; high stability; suppresses side reactions	Low single-pass conversion; clogging risk	130
Bionic 3D printed reactor	3D printed periodic structures	Optimized photon scattering; enhanced mass transfer *via* turbulence	Fabrication complexity; material limitations	103
Gas-phase reactor	Catalyst bed above liquid absorbent	Continuous product removal; shifts equilibrium forward	Humidity control required; interface stability	135

on CO selectivity, it highlights the potential of phase engineering in sulfide catalysts.[33]

CdS is another classic visible-light-driven photocatalyst, often modified to improve stability and selectivity. Biological synthesis routes offer a novel approach for creating stable composites. Gawal *et al.* utilized a vegetal route to synthesize Carbon Quantum Dots (CQDs)/CdS nanocomposites.[34] The CQDs improved charge separation and increased CO_2 adsorption capacity by 3.89 times, achieving a remarkable methanol yield of 1060.52 μmol g^{-1} h^{-1} with an apparent quantum efficiency of 7%. In terms of complex structural design, Cheng *et al.* developed a CdS/ZnS quantum dot sensitized TiO_2 nanotube array (TNTA).[35] This composite structure broadened the visible light response and achieved a methanol yield of 255.49 nmol cm^{-2} h^{-1}, demonstrating the effectiveness of combining sulfides with oxide supports. Moreover, regulating active sites in multi-component sulfides can tune product selectivity. Luo *et al.* introduced dual active sites (Cu^{2+} and Ni^{2+}) into $Zn_{0.5}Cd_{0.5}S$.[36] While their primary target was syngas, the study provided deep insights into how different metal sites reduce reaction barriers for specific intermediates (lowering ΔG for *COOH *via* Cu sites), a strategy applicable to methanol synthesis.

Bi_2S_3 and ternary sulfides are gaining attention for their narrow bandgaps. Constructing S-scheme heterojunctions is a powerful strategy to boost redox capability. Sun *et al.* fabricated a $Bi_2S_3/CdIn_2S_4$ S-scheme heterojunction. The internal electric field facilitated efficient charge transfer, resulting in a methyl formate production rate 29 times higher than pure Bi_2S_3.[37] Although the product was an ester, the mechanism explicitly revealed the pathway of CO_2 reduction to methanol as a key intermediate step.

Beyond powder catalysts, integrating metal sulfides into membrane reactors represents a significant step towards practical application. Baniamer *et al.* developed a PEBAX-1657/PES-($BiFeO_3$@ZnS) photocatalytic membrane.[38] The p–n junction between $BiFeO_3$ and ZnS promoted charge separation, while the membrane structure allowed for simultaneous CO_2 separation and photoreduction, yielding a methanol concentration of 0.85 mmol L^{-1} under UV irradiation. Additionally, Yusop *et al.* explored MgS-doped TiO_2 *via* a hydrothermal method, where optimal 0.5 wt% MgS loading achieved a methanol yield of 229.1 μmol g^{-1} h^{-1}, further validating the versatility of sulfides as dopants/co-catalysts.[39]

Although metal sulfides have shown great potential in methanol production, the stability issue remains a key bottleneck. This problem is mainly attributed to the photodegradation phenomenon caused by the oxidation of S^{2-} by photogenerated holes. Forming heterojunctions, especially Z-scheme or S-scheme structures, and combining with carbon materials such as quantum dots or graphene is the most effective strategy to alleviate this problem. These methods work by rapidly extracting holes from the valence band of the sulfide semiconductor. Additionally, a product-oriented design approach needs to be adopted. Many sulfide catalysts tend to produce CO or H_2. Therefore, to achieve high selectivity for methanol, precise control of the carbon–oxygen bond retention and the hydrogenation step is required.

3.1.1.3. Metal selenides. The application of metal selenides in the photocatalytic reduction of CO_2 to methanol is still rare, and it has shown remarkable performance in photoelectrocatalytic hydrogen production.[40] Among them, only ZnSe,[41] CdSe,[42] and WSe_2 (ref. 43) have been reported to be used in the field of methanol conversion to construct hybrid photocatalysts in combination with functional materials or other semiconductors. Metal tellurides such as ZnTe and CoTe have also been explored for the photocatalytic reduction of hydrocarbon fuels from CO_2, but have not been extended to methanol production. The reason is the sulfur compounds, selenides and tellurides, are rarely applied to CO_2 photoreduction for methanol production due to the limitation of their energy bandwidth or energy band morphology. However, most sulfur compounds such as Cu/Cu_2S, ZnSe, $CoSe_2$, ZnTe, and CoTe could still be promising for applications as long as they are modified by appropriate strategies, such as loading co-catalysts or designing heterojunctions.

The visible light response of traditional photocatalytic materials is weak, and the light source is mostly ultraviolet light

with high production cost. In order to realize the visible light response of photoelectrodes and improve the selectivity of methanol, domestic and foreign research scholars have made a lot of attempts. Recent studies have shown that in metal-nonmetal compounds, such as metal oxides, sulfides, selenides, *etc.*, the attraction of metals and nonmetals for C and O is different, which suggests that there is also an inhomogeneity of their attraction for intermediates in CO_2 reduction, which is conducive to the enhancement of the selectivity of high-value fuels, such as methanol, by adjusting the attraction of intermediates.[44–50] Cu-based materials, among metal-nonmetal compounds, have an excellent position in photocatalytic CO_2 reduction (CO_2RR) technology, especially in the generation of high-value fuels, and Cu-based materials are one of the most suitable materials available.[51–54] In addition, metal selenides tend to have better catalytic activity for CO_2 in CO_2 reduction applications compared to the more studied oxides and sulfides of the same family, mainly due to the ability of unsaturated selenium atoms to increase the number of exposed active sites used for CO_2 conversion, as well as the ability to enhance both conductivity and selectivity.[55–58]

Therefore, Cu-based materials tend to have highly efficient catalytic performance and excellent electrical conductivity and stability. On this basis, $Cu_{2-x}Se$ have also been successively prepared for photocatalytic CO_2 reduction, and very excellent results have been achieved. This indicates that Cu-based catalysts will also have excellent prospects in CO_2 reduction.[59,60] However, single-metal catalysts are often accompanied by CO production in the CO_2RR reaction, which results in a decrease in the selectivity of high-value fuels such as methanol. On this basis, bimetallic-based catalysts, by virtue of their M_1–C–O–M_2 configuration, are able to greatly inhibit CO production, which is expected to improve the selectivity of high-value fuels such as methanol. In addition, the Cu-based material itself has a suitable band gap that enables visible light response, which is necessary for the utilization of sunlight.[61–63]

3.1.2. Metal–organic frameworks (MOFs). Metal–Organic Frameworks (MOFs), characterized by their tunable porous structures and diverse metal–ligand combinations, offer a versatile platform for photocatalytic CO_2 reduction. However, pristine MOFs often face limitations such as rapid charge recombination and limited visible light absorption. To address these issues, constructing heterojunctions by integrating functional guests into the MOF matrix has become a primary strategy. For instance, Sonowal *et al.* developed a g-CNQDs@NH_2-UiO-66 composite by incorporating graphitic carbon nitride quantum dots (g-CNQDs). This design not only retained the MOF's porous structure but also established a Z-scheme heterojunction, where the g-CNQDs extended the light absorption range and the internal electric field facilitated efficient charge separation, achieving a high methanol yield of 9264 μmol g^{-1}.[64] Similarly, Rameshwar *et al.* synthesized a ternary CuO-rGO/Ag-CuBDC nanocomposite *via* a green method. By introducing Ag nanoparticles and reduced graphene oxide (rGO) into the CuBDC framework, they utilized the Schottky junction effect of Ag to trap electrons and the conductive rGO network to accelerate electron transfer. This synergy significantly boosted the methanol production rate to 30.49 μmol g^{-1} L^{-1} under LED irradiation, far surpassing single-component counterparts.[65] These studies underscore that the modular nature of MOFs makes them ideal hosts for engineering localized charge-transfer pathways.

Beyond serving as photocatalytic hosts, MOFs can also act as precursors for synthesizing robust metal/carbon heterostructures or defective metal oxides through controlled pyrolysis. This "MOF-derivation" strategy allows for the inheritance of the MOF's original morphology while introducing active sites like defects or metal–support interfaces. Zhang *et al.* utilized waste CuBTC MOFs to prepare a bimetallic Ni–Cu/C catalyst *via* adsorption-pyrolysis. The Ni doping optimized charge transfer kinetics and lowered the activation energy for intermediates, achieving highly selective CO_2 reduction with excellent stability.[66] In another approach targeting methanol selectivity, Zhang *et al.* transformed MIL-125(Ti) into defective TiO_2 oval nanocages anchored with Cu nanoparticles (8Cu/H–TiO_2). The resulting Schottky junctions and oxygen vacancies, derived from the MOF precursor, worked synergistically to enhance CO production, although fine-tuning selectivity towards methanol in such derived oxides remains a challenge.[67] From a perspective of sustainability, transforming spent or waste MOFs into high-value photocatalysts not only addresses waste management but also provides a cost-effective route for scalable catalyst production.

While heterojunction construction and derivative strategies are effective, the intrinsic design of the MOF structure itself represents the frontier of atomic-level precision control. A particularly innovative direction is the engineering of intramolecular electron transfer pathways within a single MOF framework. Zhao *et al.* demonstrated this by constructing an asymmetric "intramolecular electron compartment" (IEC) within a Cu-MOF (Cu-MOF-NK1). By creating a gradient of electron accumulation between adjacent copper rings, they achieved a directional cascade electron transfer, enabling the multi-electron reduction of CO_2 to methanol with a remarkable yield of 115.8 μmol g^{-1} h^{-1} and 92.0% selectivity, even without sacrificial agents.[68] This work highlights a critical insight: achieving high selectivity for multi-electron products like methanol demands more than just charge separation; it requires precise management of electron density at the active site. Future reactor designs should integrate these advanced MOFs, particularly those with directional electron transfer capabilities, into continuous-flow microreactors. This integration could stabilize reaction intermediates by optimizing the local concentration of reactants and removing products promptly, thereby bridging the gap between mechanistic elegance and practical methanol production efficiency.

3.1.3. Non-metal-based catalysts. Non-metal-based catalysts are widely used in photocatalysis, but they have unavoidable drawbacks, such as high cost and poor durability. The importance of studying non-metallic-based catalysts is increasing due to the poisoning problems that may be caused. These non-metallic-based catalysts contain a variety of rare earth elements, which have the advantages of being inexpensive, environmentally friendly and effective in transferring

electrons. With the advancement of science and technology, the types of these catalysts have been increasing, among which the most common ones are carbon-based materials, phosphorus-based materials, and silicon carbide.[69] The one-dimensional structure of carbon nanotubes endows them with high conductivity, excellent electron mobility, and large specific surface area. Meanwhile, this type of material has achieved relatively low-cost macroscopic preparation. Therefore, it is regarded as a key component for making various types of functional composites. Semiconductor photocatalysts based on graphene[70] have attracted much attention due to their universality in environmental and energy applications. Graphitic carbon nitride (g-C_3N_4) is an important non-metal-based catalyst for solar energy conversion to fuel,[71] narrow band gap (2.7 eV) and negative conduction band potential (−1.12 eV), so g-C_3N_4 plays an important role in photocatalytic reduction of CO_2. However, g-C_3N_4 also has many drawbacks, mainly in the form of larger particle size and faster photogenerated electron–hole pair complexation, which further reduces the electron utilization of g-C_3N_4 in the reduction of CO_2, and we could modify it by using the aforementioned means, such as exfoliation, elemental doping, metal deposition, semiconductor coupling, and protonation, *etc.*

3.2. Performance optimization strategies for photocatalysts

Existing photocatalysts are more or less affected by their inherent defects, which prevent them from exerting their optimal photocatalytic performance. In this regard, many strategies have been attempted to design or improve photocatalysts to enhance their catalytic performance, such as ion doping, micromorphology design, defect engineering, and so on. By studying the photocatalytic reduction of CO_2 to methanol in recent years, the design strategies of related photocatalysts are sorted out.[63]

3.2.1. Bandgap modulation *via* doping. The photocatalytic performance of most semiconductors is limited by their own imperfect band structure, which determines the material's light absorption ability and carrier generation efficiency.[72] As mentioned above, although a smaller photocatalyst band gap facilitates the utilization of the solar spectrum, it is not conducive to meeting the overpotential required for redox reactions. Therefore, the undesirable band gap of semiconductors in the photocatalytic reduction of methanol by CO_2 was modified by adjusting the energy band structure through ion doping to improve the spectral response region and enhance the photocatalytic performance. It should be noted that cation doping has a more general effect on the adjustment of the CB side and anion doping has a more general effect on the VB side.[13] In order to adjust the inherent undesirable energy band structure of semiconductors, ion doping is undoubtedly valuable for the development of methanol-selective photocatalysts, which makes them highly sought after.

3.2.2. Microscopic morphology. Micromorphology design effectively avoids the obstacles of rapid complex recombination of photogenerated charges, thus facilitating the development of high-performance photocatalysts. Various forms of nanophotocatalysts have been widely reported for photocatalytic reduction of CO_2,[73] such as nanoparticles/MXene quantum dots (0D), nanorods/nanowires/nanofibers (1D), nanosheets/nanoplates (2D), and nanospheres/nanoflowers (3D). The micromorphology design shortens the diffusion distance of photogenerated charges, which facilitates interfacial charge transfer while preventing the complexation of photogenerated electrons. Meanwhile, the design amplified the pore size and specific surface area of the photocatalysts, which enhanced the CO_2 adsorption on their surfaces.

Compared with one- and two-dimensional materials, more complex and interconnected three-dimensional layered materials, such as core–shell, hollow, and multi-shell structures, which are mainly constructed from basic materials such as nanoparticles, nanorods, and nanosheets, have been more widely developed. Zheng *et al.*[74] synthesized nano-silver-decorated flower-like molybdenum disulfide nanosheets for the CO_2 photocatalytic reduction, with a methanol yield of up to 365.08 μmol g^{-1} h^{-1}. It was pointed out that the phase transition of molybdenum disulfide from one to two dimensions realized the broadening of its band gap, which is instructive for related studies. Prajapati and coworkers[75] synthesized Ni/NiO semiconductors with core–shell structure and grafted cobalt phthalocyanine (CoPc) on them to synthesize novel nanocomposites for methanol production by CO_2 photocatalytic reduction. The methanol conversion of this photocatalyst was 151.7 μmol g^{-1} h^{-1}, and the results showed that the catalyst had excellent recoverability and stability. The microformal design implies higher surface area, more active sites, better CO_2 adsorption capacity and more effective carrier separation, which can significantly improve the photocatalytic performance and is of great practical significance for photocatalysts for the reduction of CO_2 to methanol.

3.2.3. Heterojunction construction. Heterojunction design that favors the spatial separation of photogenerated electron–hole pairs is a promising option for the preparation of excellent photocatalysis. As the most feasible heterojunction for improving CO_2 photoreduction efficiency, type II heterojunction is further subdivided into four types, namely conventional type II heterojunction, p–n heterojunction, Z-type heterojunction, S-type heterojunction and surface heterojunction.

As an effective means to hinder photogenerated charge complexation,[76] p-type semiconductors and n-type semiconductors construct p–n heterojunctions with internal electric fields. Taking the n-type semiconductor ZnO as an example, Taraka *et al.*[77] prepared CuO/ZnO p–n heterojunctions for the photocatalytic reduction of CO_2 to methanol, which exhibited enhanced photogenerated charge separation. The yield of this photocatalyst was 3855.36 μmol g^{-1} h^{-1} in aqueous solution of dimethylformamide (DMF) and triethylamine (TEA) for 24 h of reaction. The methanol yield of this catalyst was significantly higher compared to that of pure ZnO, and this result strongly confirms the promising potential of the heterostructure in suppressing the rapid recombination of electron–hole pairs and enhancing the rate of photogenerated charge transfer.

3.2.4. Defect engineering. By tuning the interaction of defects on photocatalysts with reactive molecules, the activation energy can be reduced and the reaction pathways can be altered. Therefore, tuning of surface defects (changing their type and density) is an effective method to enhance the performance of photocatalysts. Effective progress has been made in the study of vacancy defects in semiconductor materials.[78] Zhu *et al.*[79] developed CeO_2 (110) and CeO_2 (100) cuts for CO_2 photocatalytic reduction based on abundant oxygen (Lewis acidity) and hydroxyl (Lewis alkalinity) defects on the surface of CeO_2, which is highly susceptible to surface oxygen vacancies. The experimental results show that oxygen vacancies are easily generated on CeO_2 (110) compared to CeO_2 (100), resulting in better visible light response and faster carrier migration of CeO_2 (100). Combining the experimental results with DFT calculations, they observed that the surface of CeO_2 (110) is richer in OH species, which provides more electron density (*i.e.*, Lewis alkalinity). In addition, CeO_2(110) is more favorable than CeO_2(100) for the adsorption and activation of CO_2 molecules, resulting in the generation of carboxylate states and $*CO_2^-$, rather than carbonates, on it. Oxygen vacancies have a dynamic role in promoting charge migration rather than recombination sites and are key factors in facilitating the reduction of CO_2 to C1–C2 hydrocarbons. Anion and oxygen defect synergism also contributes to future explorations.

3.2.5. Co-catalyst loading. Loading co-catalysts on photocatalysts to transfer electrons is a common and effective scheme to assist surface charge transfer and inhibit photogenerated charge complexation. It mainly attenuates photocorrosion by depleting the photogenerated charge on the co-catalyst and improves the performance of the photocatalyst. In addition, the co-catalyst plays an important role in the adsorption/activation of CO_2 molecules and the formation of reaction intermediates, which significantly affects the photocatalytic activity and product selectivity. Precious metals (*e.g.*, Ag, Pt, Au, Pd, Ru, Rh), non-precious metals (*e.g.*, Cu, Zn, Ni), and corresponding oxides are the most commonly used co-catalysts in CO_2 photocatalytic reduction. The requirement for metals and corresponding oxides as co-catalysts is that their Fermi energy levels are lower than the edge of the semiconductor CB in order to establish a Schottky barrier at the contact interface.[80]

Notably, although precious metal (*e.g.*, Ag, Pt, Au, Ru, Rh) co-catalysts have been reported to significantly promote the activation of CO_2 molecules, their expensive cost and limited reserves severely limit their large-scale applications. SACs (Single-Atom Catalysts) can also effectively overcome the relatively poor catalytic performance and expensive cost due to the limited number of precious metal active sites exposed on the surface of photocatalysts.[81] Currently, SACs have received extensive attention in the field of noble metal materials, and their great potential for the photocatalytic reduction of methanol by CO_2 is undeniable, which means that more related literature can be expected in the future.[82]

The results obtained through various performance optimization strategies are shown in Table 1. The C–TiO_2, N–TiO_2 catalysts were doped with non-metallic elements through the strategy of doping the CB side of the catalysts, which improved the yield of HCOOH and CH_3OH.[83,84] The Co–TiO_2, In–TiO_2 catalysts were doped with transition metal elements through the strategy of doping the CB side of the catalysts, and the catalytic performance of the catalysts was optimized.[85,86] The Ag–TiO_2 catalysts significantly promoted the activation of CO_2 molecules through the introduction of precious metal co-catalysts, which substantially improved the photocatalytic performance of the catalysts.[87] The $FeTiO_3/TiO_2$ and CdS/TiO_2 catalysts were designed by constructing heterojunctions at the interface of the two catalytic materials to improve the catalytic performance of the composite catalysts, and the heterojunctions were optimized to enhance the photogenerated electron yield of the composite catalysts.[88,89] The design of heterojunction can optimize the enrichment of photogenerated electrons in the composite catalyst for the transfer, and substantially improve the catalytic performance.

High-performance catalysts need to have high photocatalytic activity, stability and suitable visible light absorption range. In the past, semiconductor oxides and sulfides were mainly used as the research objects of photocatalysts. However, these semiconductor oxides and sulfides have the disadvantages of difficult modification, photocorrosion, poor light absorption performance and acid and alkali resistance, which largely restricted the industrial application of photoelectrocatalysis, and the new photoelectrocatalytic materials have become the hot spots in the field of photocatalysis. In recent years, although many scholars[90–92] have been devoted to the research and development of new photoelectrocatalysts, there are not many catalysts that really meet the high performance standards. Therefore, it is of great practical significance to modify the existing catalyst materials by surface modification, structure optimization, doping or compounding[93,94] to improve the performance of the catalysts as well as to develop new and efficient photoelectrocatalytic materials.[95,96]

4. Practical application and engineering of photocatalytic CO_2 reduction reactors

The transition of CO_2RR from laboratory curiosity to industrial viability is contingent not only on catalyst performance but fundamentally on reactor engineering. High-performance catalysts often fail to replicate their intrinsic activity in macroscopic systems due to heat/mass transfer limitations, inefficient photon utilization, and product back-reaction. This section critically analyzes the evolution of reactor designs, moving from the limitations of conventional systems to process intensification strategies in coupled reactors and emerging optofluidic microreactors. We emphasize design principles, technical challenges, and representative solutions supported by recent engineering advancements.

4.1. Reactor design principles

4.1.1. Suspension reactor and fixed bed reactor. Conventional photocatalytic reactors are generally categorized into

slurry and immobilized systems, alongside emerging membrane configurations (Fig. 3).[97] The fundamental design philosophy revolves around maximizing photon utilization and reactant-catalyst contact. However, macro-scale engineering analysis reveals inherent bottlenecks in these configurations.

In slurry systems (Fig. 3A), catalyst microparticles are dispersed in the liquid phase. While active particle motion minimizes mass transfer resistance at the liquid–solid interface, these reactors suffer from severe photon transport attenuation. According to the Beer–Lambert law, light intensity decays exponentially with depth, creating a "dark zone" in the reactor core where catalysts remain inactive.[98] To mitigate this, Wang *et al.* utilized CFD simulations for a continuous stirred tank reactor (CSTR) to demonstrate that optimizing macroscopic flow convection and mesoscopic diffusion can significantly compress the diffusion layer to ~60 μm, thus enhancing local mass transfer.[99] Despite these fluidic optimizations, the energy-intensive downstream separation of nano-photocatalysts remains a practical hurdle.

Immobilizing catalysts on substrates (Fig. 3B) resolves recycling issues but introduces substantial mass transfer resistance and light shielding. Common designs include fiber-optic reactors and multi-channel honeycomb reactors.[100,101] To address optical inefficiencies, Mehrpooya *et al.* demonstrated that optimizing the internal layout of fiber-optic reactors could improve spatial light distribution, increasing methanol yield by 60% compared to single-fiber designs.[102] Similarly, to overcome the opacity of conventional honeycomb monoliths, Pan *et al.* fabricated a 3D-printed "fence-like" cell reactor.[103] Its bionic geometry optimized photon scattering and reactant flow, significantly outperforming traditional designs. Nevertheless, in these immobilized systems, the diffusion of CO_2 from the bulk liquid to the catalyst surface remains the primary rate-limiting step.

4.1.2. Reaction medium-driven reactor design. The design of a photocatalytic reactor must be fundamentally tailored to the reaction medium, as the underlying kinetic challenges and mass transfer mechanisms differ drastically between liquid-phase and gas-phase systems.

4.1.2.1. Liquid phase photocatalytic reactors. Traditionally, most studies have been performed in liquid-phase slurry systems or immobilized reactors. Common media include aqueous solutions and organic solvents such as DMF or TEOA. The mechanistic advantage of liquid systems lies in the abundant supply of protons (H^+) derived from water, which is essential for the 6-electron reduction to methanol. However, CO_2 exhibits extremely low solubility in water. The solubility reaches approximately 33 mM under standard conditions. This phenomenon creates severe mass transfer resistance across the gas liquid solid interface and becomes the major bottleneck of the reaction system. Consequently, the thermodynamically favored HER often outcompetes CO_2RR. To overcome this, reactor design has pivoted towards enhancing local CO_2 concentration. Strategies include operating under elevated pressures to thermodynamically drive CO_2 dissolution.[104] The Ebri research team designed a dedicated reactor for high-pressure and supercritical CO_2 conditions.[105] The reactor adopts stainless steel as the main body and is equipped with sapphire windows from Rayotek 101060. The device can withstand extreme operating pressure up to 78 bar and a working temperature of 70 °C. Under a 60 bar high-pressure CO_2 condition, the CO production rate increased 125 times compared to the 3 bar low-pressure condition.

Moreover, advanced reactor designs incorporate hydrophobic interfaces, such as PTFE membranes or catalyst surface modifications. These interfacial modifications aim to construct a highly efficient triphase boundary that directly addresses the low solubility issue while steering the reaction pathway. For instance, Wang *et al.* developed a self-supporting triphase photocatalytic microreactor by engineering a core–shell structure (NAL-MRF) with tunable wettability.[106] By integrating a hydrophobic melamine–resorcinol–formaldehyde (MRF) component to capture gaseous CO_2 and a hydrophilic NiAl layered double hydroxide (NAL) component to ensure water supply, this dual-wetting design perfectly balanced CO_2 mass transfer and proton provision. Consequently, it effectively suppressed the competitive HER, achieving a remarkable methanol yield of 31.41 μmol g^{-1} h^{-1} with over 93% selectivity. Beyond merely improving reactant mass transfer, wettability engineering can also shift the reaction equilibrium. Lu *et al.* demonstrated this by applying an alkylsilane coating to In_2O_3 for solar-driven methanol synthesis.[107] The rationally designed hydrophobic layer effectively repelled polar products from the catalyst surface, preventing product accumulation and thermodynamically driving the reaction forward. Accompanied by the hydrogen-donating ability of the alkyl chains, the optimized catalyst achieved a superior methanol production rate of 1436 μmol g_{cat}^{-1} h^{-1}. Similarly, in photoelectrochemical liquid systems, tailoring the electrode microenvironment *via* hydrophobic coatings has proven highly effective in manipulating intermediate dynamics. Shang *et al.* designed a silicon micropillar array electrode coated with a superhydrophobic fluorocarbon (CF_x) layer.[108] This unique interfacial architecture not only prevented electrolyte flooding to facilitate CO_2 transport but also efficiently trapped the crucial reaction intermediate (*CO), thereby significantly increasing its local concentration. As a result, the faradaic efficiency for deep reduction to methanol reached an impressive 20%, highlighting the critical role of surface wettability in bridging microscopic kinetics and macroscopic reactor performance.

4.1.2.2. Gas phase photocatalytic reactors. In stark contrast to liquid-phase systems, gas-phase photocatalytic CO_2 reduction typically operates in continuous-flow fixed-bed, monolithic, or membrane reactors, where gaseous CO_2 and water vapor act as the primary reactants. The intrinsic mechanistic advantage of the gas-phase configuration is the complete elimination of the CO_2 solubility limit. By directly exposing the photocatalyst to a gaseous stream, the gas–solid mass transfer resistance is drastically minimized, ensuring an extremely high local CO_2 concentration at the active sites. Furthermore, water exists merely in the vapor state within the reaction system. The restricted presence of water fundamentally alters the surface proton kinetics, which inherently suppresses the competitive and thermodynamically favored liquid-phase HER, theoretically

making it easier to steer the selectivity toward carbon-based products. However, transitioning to a gas-phase medium introduces a distinct set of kinetic and reactor engineering challenges. The foremost obstacle originates from the proton starvation effect. Since the deep reduction of CO_2 to methanol requires six protons, an insufficient partial pressure of water vapor can severely choke the reaction kinetics, trapping intermediates and favoring the 2-electron reduction to CO. Conversely, excessive humidity can lead to capillary condensation of water within the catalyst pores, blocking active sites and ironically re-introducing liquid-phase mass transfer limits.

Another critical bottleneck specific to gas-phase methanol synthesis is product desorption. Methanol is highly polar and has a higher boiling point than byproducts like CO or CH_4. In a traditional gas–solid reactor, newly formed methanol molecules tend to strongly bind to the catalyst surface. If not rapidly evacuated, they act as a poison by occupying active sites, or worse, undergo reverse-oxidation by photogenerated holes back to CO_2 or HCHO. To navigate these challenges, modern gas-phase reactor design has pivoted towards precise humidity control, flow dynamics optimization, and rapid product extraction. For instance, Pomilla *et al.* systematically investigated the effects of the mole ratio of H_2O/CO_2 feed and the contact time in the continuous photocatalytic membrane reactor. They found that maintaining a H_2O/CO_2 feed mole ratio of 5 and a contact time of 2 s was the optimal condition, which was crucial for balancing the proton supply and CO_2 adsorption. This precise regulation was promoted by the continuous operation mode, facilitating the rapid removal of products, reducing the oxidation and secondary reactions of methanol and ethanol, and avoiding catalyst agglomeration. Ultimately, a methanol production rate of 17.9 μmol g^{-1} h^{-1} and a total conversion carbon efficiency of 47.6 μmol g^{-1} h^{-1} were achieved.[109] To directly address the methanol desorption issue, advanced reactor architectures have integrated continuous extraction mechanisms. Felix Rechberger and Markus Niederberger, among others, have designed a novel continuous-flow reactor.[110] This reactor combines a highly porous TiO_2–Au nanoparticle-based aerogel structure with a continuous carrier gas flow. Through optimizing the gas flow path, this design enables the reaction gas to uniformly pass through the three-dimensional porous network of the aerogel, promptly removing the generated methanol vapor from the catalyst surface and reducing its retention time at the active sites. The high porosity and large specific surface area of the aerogel facilitate gas diffusion, further accelerating the desorption of methanol from the catalyst surface. Compared with traditional powder or film-type catalysts, this design achieves selective photo-reduction of CO_2 to methanol with a conversion rate of 2.58 μmol g^{-1} h^{-1}, without the formation of by-products such as CO, formic acid, or methane, demonstrating extremely high product selectivity.

Crucially, because gases possess significantly lower thermal conductivity than liquids, gas-phase reactors are exceptionally well-suited for integration with concentrated sunlight and thermal management strategies. As localized heat cannot be easily dissipated by the gaseous medium, photothermal synergistic effects can be maximized. Mirzaei *et al.* designed a photothermal gas-phase reactor that incorporated a TiO_2/1% NiO–$InTaO_4$ catalyst coating on a filled monolithic-fiber bed.[111] By concentrating the solar photon flux, this reactor achieved optimized control of the local bed temperature to 365 K. This not only accelerated the rate-determining hydrogenation step but also thermodynamically promoted the rapid desorption of methanol molecules from the catalyst surface. This thermal management strategy effectively bypassed the kinetic trap of the $*OCH_3$ intermediate and achieved a significant catalyst-to-methanol yield ratio (CSMP) of 16 374 μmol g^{-1} h^{-1}.

4.2. Photo-thermal/electrochemical coupled reactors

To overcome the thermodynamic barriers and slow kinetics of pure photocatalysis, integrating external energy fields, specifically thermal and electrical energy, has emerged as a robust solution. By applying an external bias potential, photoelectrocatalytic (PEC) reactors effectively suppress the recombination of photogenerated electron–hole pairs.[112] While traditional PEC reactors often face challenges such as low mass transfer efficiency and substantial ohmic drops,[113] recent innovations have focused on structural optimization to mitigate these issues. For example, the turntable photoelectrocatalytic liquid membrane reactor developed by Xu *et al.*[114] and the corrugated plate reactor by Zhang *et al.*[115] significantly improve both light utilization and mass transfer. To address the persistent challenge of product recombination in single-pot reactors, Lin *et al.* proposed a novel twin reactor design that physically separates the CO_2 reduction and water oxidation half-reactions into two distinct chambers connected by a Fe^{2+}/Fe^{3+} redox mediator.[116] By incorporating a triphase interface using a hydrophobic PTFE membrane, they achieved a CO_2 reduction rate of 48.2 μmol g^{-1} h^{-1}, approximately 5 times higher than conventional single-phase reactors, while effectively suppressing reverse reactions. Furthermore, integrating enzymatic catalysis offers exceptional product selectivity. Lim *et al.* reviewed enzyme-membrane reactors (EMR) where photocatalytic NADH regeneration is seamlessly coupled with enzymatic CO_2 reduction.[117] Utilizing a hollow fiber membrane reactor within this integrated system boosted formic acid yield up to 1.04 mM h^{-1} compared to non-integrated setups.

Parallel to PEC systems, photothermal reactors utilize the synergistic coupling of photon and thermal energy to break kinetic bottlenecks. By incorporating plasmonic metals or broadband absorbers like $SrTiO_3$–Cu–TiN, these systems harness the full solar spectrum to create localized hot spots, thereby lowering the activation energy for surface reactions.[118,119] From an engineering perspective, continuous-flow photothermal reactors employing microchannels or porous media inherently intensify interfacial contact and allow precise control over reactant residence time.[120] Additionally, structural designs utilizing capillary wicking enable *in situ* water evaporation, ensuring a balanced supply of steam and CO_2 while simultaneously preventing catalyst poisoning, which has extended operational stability beyond 500 hours.[121]

While these conventional photothermal designs significantly improve reaction rates, driving the complex 6-electron reduction to methanol requires a more fundamental leap in energy input. Under standard 1-sun (AM 1.5 G, 100 mW cm^{-2}) illumination, the intrinsically low photon flux limits multi-electron accumulation on the catalyst surface, often stalling the reaction at the 2-electron reduction stage to produce CO. To bridge this gap, integrating concentrated solar irradiation with precise thermal management has emerged as a cutting-edge reactor engineering strategy. Optical concentrators such as Fresnel lenses exponentially amplify the photon flux by tens to hundreds of suns, dramatically boosting the surface charge density necessary for sluggish C–O cleavage and C–H bond formation. However, concentrating sunlight inevitably generates intense localized heating from infrared (IR) absorption and non-radiative relaxation. If unmanaged, this excess thermal energy can cause severe catalyst deactivation *via* sintering or thermodynamically shift the selectivity toward undesired byproducts like CO or CH_4. Conversely, if properly harnessed, this synergistic local heating accelerates intermediate hydrogenation and promotes the rapid desorption of highly polar methanol molecules before they undergo over-oxidation.

Therefore, the successful implementation of concentrated solar photothermal reactors demands meticulous macroscopic engineering to balance light distribution and thermal gradients.[122] Traditional flat-bed reactors are highly inefficient under concentrated light due to severe surface effects, leaving the bulk material cold and inactive. To mitigate this, advanced reactor designs incorporate 3D macroscopic structures and volumetric light absorbers. For instance, Xu *et al.* developed a three-dimensional porous titanium foam photothermal reactor, which can achieve deep light penetration and uniform volumetric heating under 10.6 times concentrated illumination, thereby significantly improving the solar energy utilization efficiency and CO_2 conversion rate.[123] Ultimately, this strategic integration of advanced 3D structural engineering and concentrated solar irradiation at the reactor level effectively maximizes the synergistic photothermal effects, representing a highly promising pathway toward the industrial-scale production of "liquid sunshine".

4.3. Intensification *via* optofluidic microreactors

Microreactors represent a paradigm shift in reactor engineering, leveraging microscale flow phenomena to achieve process intensification. Defined by a characteristic hydraulic diameter (D_h) of less than 1 mm, microreactors offer extraordinary heat and mass transfer capacities. Unlike conventional reactors with surface-area-to-volume (S/V) ratios of 50–500 m^{-1}, microreactors can achieve ratios exceeding 10 000 m^{-1}. As illustrated in Fig. 4, microreactors have evolved into various structural forms to optimize contact area and photon transfer, including multi-capillary, single-channel, multiphase, and coil-type designs.[124–127]

4.3.1. Mass transfer and photon transport optimization. In microchannels, the flow is typically laminar with a low Reynolds number, where transport is dominated by diffusion rather than turbulence. While this might seem disadvantageous, the ultra-short diffusion distances ranging from 10 to 100 μm ensure rapid reactant supply to the catalyst surface.

Crucially, microreactors resolve the photon transport bottleneck. The channel depth is usually smaller than the photon penetration depth, ensuring that the entire reaction volume is uniformly illuminated under the optically thin condition. To further enhance this, Ola and Maroto-Valer developed a photocatalytic monolithic microreactor (Fig. 5), where optical fibers are threaded through a ceramic honeycomb structure.[128] Similarly, to address the low throughput of single microchannels, Tahir *et al.* developed a V_2AlC-mediated Z-scheme heterojunction catalyst supported on a honeycomb monolith.[129] This configuration achieved the highest overall efficiency among tested reactors, with remarkably high yields of CO, CH_4, and H_2 reaching 49 313, 32 429, and 14 060 μmol g^{-1} respectively. The improved performance is attributed to optimized light distribution and mass transfer within the thin catalyst coatings.

4.3.2. Emerging microreactor configurations and strategies. Despite their advantages, early microreactors faced challenges such as clogging, low throughput, and difficulties in gas–liquid separation. Recent innovations have provided targeted solutions.

4.3.2.1. Optimization of operation mode. The choice between continuous flow and batch operation profoundly influences product selectivity. Tahir *et al.* conducted a comparative study using a 2D/2D $ZnCo_2O_4$/pg-C_3N_4 heterojunction catalyst.[130] They found that continuous flow favored stable CO production (3.76 μmol g^{-1} h^{-1}) with low CH_4 selectivity due to short residence time preventing further hydrogenation. In contrast, batch reactors allowed for product accumulation, achieving a remarkably high CO yield of 616 μmol g^{-1} h^{-1} and enabling deep reduction to CH_4. This highlights that reactor operation mode is a tunable parameter for controlling product distribution. Optimization of operating parameters is also critical. Nabil *et al.* systematically investigated parameters in a meso-scale continuous-flow photoreactor, finding that a flow rate of 500 μL min^{-1} and temperature of 30–40 °C were optimal for methanol production using Pt/TiO_2/RGO composites.[131]

4.3.2.2. Solving gas solubility limits. The low solubility of CO_2 in aqueous electrolytes limits the reaction rate. Traditional single-layer membrane reactors (Fig. 6a) often suffer from gas precipitation issues.[132,133] Albo *et al.* proposed a double-layer transport mode (Fig. 6b) using a gas-permeable, hydrophobic membrane.[134] Moving beyond liquid-phase limitations entirely, Morawski *et al.* introduced a novel gas-phase reactor where the photocatalyst bed composed of TiO_2 supported on glass fiber was positioned above the water surface.[135] This allowed gaseous N_2 and CO_2 to react, with generated ammonia and organic products continuously absorbed into the water, driving the equilibrium forward and resulting in millimolar-level production.

4.3.2.3. Solving product separation. In single-channel reactors, liquid products (methanol) mix with reactants and can be re-oxidized by O_2 evolved at the anode. Dual-chamber microreactors separate the oxidation and reduction half-reactions using a proton exchange membrane (PEM). Albo *et al.* demonstrated that such a continuous flow setup with Cu–TiO_2

catalysts could continuously extract methanol, preventing product accumulation and degradation.[134]

4.3.2.4. Coupling with biological/fuel cell systems. To further enhance efficiency and utility, hybrid systems are emerging. Xie *et al.* designed a coupled system integrating CO_2 reduction with a Photocatalytic fuel cell.[136] Additionally, Sakimoto *et al.* and Zhang *et al.* have explored bio-hybrid microreactors, integrating non-photosynthetic bacteria with inorganic photocatalysts to achieve highly selective conversion of CO_2 to acetic acid.[137,138] Table 2 provides a comparative summary of these advanced reactor configurations.

5. Conclusion and perspectives

Current research has successfully established that selectivity toward methanol, a six-electron transfer process, remains the primary kinetic challenge. It often competes with the thermodynamically favored two-electron reduction to CO or the hydrogen evolution reaction. Although strategies such as bandgap engineering, defect construction, and Z-scheme heterojunctions have improved light absorption and charge separation, most catalysts still suffer from linear scaling relationships of intermediates, limiting the intrinsic catalytic turnover. Copper-based and bimetallic catalysts with M1-C-O-M_2 configurations have shown promise in breaking these scaling relations, yet their stability under long-term irradiation remains a concern. In addition, a significant disconnect exists between intrinsic catalyst activity and macroscopic reactor performance. For example, in conventional liquid-phase slurry reactors, mass transfer limitations caused by low CO_2 solubility and photon transport attenuation known as the dark zone effect often mask the true potential of high-performance photocatalysts. Transitioning to gas-phase continuous-flow systems effectively eliminates these solubility limits, yet it introduces new engineering challenges such as precise humidity control and rapid methanol desorption that must be carefully managed.

To propel this technology from laboratory curiosity to industrial viability, future research must shift focus from trial-and-error material synthesis to rational, multi-scale system design. We propose the following strategic directions:

5.1. Precision engineering of active sites

Future catalyst design must move beyond simple doping to atomic-level precision. The construction of dual-atom sites or frustration-Lewis-pair sites on MOFs offers a pathway to stabilize specific intermediates (*e.g.*, CH_3O) essential for methanol production while suppressing C–C coupling. Achieving a solar-to-fuel conversion efficiency exceeding 10% will likely require these advanced architectures to minimize overpotential.

5.2. Multi-field synergistic catalysis and concentrated solar engineering

Relying solely on low-intensity photon energy is often insufficient to overcome the high thermodynamic barriers of the 6-electron reduction to methanol. The integration of external fields, specifically concentrated solar photothermal and photoelectrochemical coupling, represents a robust solution. By exponentially amplifying the photon flux using optical concentrators and harnessing infrared radiation through precise dynamic thermal management, these advanced hybrid systems can effectively accelerate sluggish intermediate hydrogenation and promote rapid product desorption. This strategic decoupling of CO_2 activation thermodynamics from protonation kinetics will significantly enhance methanol yield, product selectivity, and overall system durability.

5.3. Intelligent reactor design and digitalization

The future of photoreactor engineering lies in the integration of predictive modeling and intelligent control to bridge the gap between theoretical design and practical application. As highlighted by Mehrpooya *et al.*, numerical simulations, specifically Computational Fluid Dynamics (CFD) coupled with radiation models like the Discrete Ordinate Method, are becoming indispensable for optimizing reactor geometry prior to fabrication. Based on this, future research should give priority to developing highly accurate digital twin models of reactors. These models will combine real-time sensor data with kinetic models to achieve adaptive process control. At the same time, combined with artificial intelligence-assisted design, machine learning algorithms will navigate the complex multi-parameter space of reactor design to effectively balance light distribution, fluid dynamics, and reaction kinetics.

5.4. Integrated capture and conversion (ICC)

A transformative direction is the development of smart integrated systems that couple CO_2 capture directly with conversion units. Utilizing passive flow mechanisms such as capillary forces, as demonstrated by Peña *et al.* in multiphase capillary reactors, can circumvent the energy-intensive step of compressing and purifying CO_2. This integration is crucial for decentralized application scenarios, such as converting flue gas directly into methanol at emission sources.

In conclusion, realizing the vision of a "liquid sunshine" economy requires a holistic approach that intertwines materials innovation with reactor engineering and artificial intelligence. Only by breaking the silos between these disciplines can we achieve the high efficiency, selectivity, and stability required for industrial-scale solar methanol production.

Author contributions

Cheng Zuo and Chunling Xin: writing and revising manuscript. Qian Su: conceptualization, methodology, software, investigation, writing – original draft. Jing Wang: funding, acquisition, and supervision. Qian Su: methodology, validation, formal analysis, visualization. All authors have read and agreed to the published version of the manuscript.

Conflicts of interest

The authors declare that they have no known competing financial interests or personal relationships that could have appeared to influence the work reported in this paper.

Data availability

No primary research results, software or code have been included and no new data were generated or analysed as part of this review.

Acknowledgements

Financial support for carrying out this work was provided by the Doctoral Research Foundation of Weifang University (2024BS20), the Science and Technology Development Plan Foundation of Weifang (2024GX017) and the Youth Innovation Science and Technology Support Program for Higher Education Institutions in Shandong Province, China (2025KJG042).

References

1 X. L. Zhu, H. B. Zong, C. J. V. Pérez, H. H. Miao, W. Sun, Z. M. Yuan, S. H. Wang, G. X. Zeng, H. Xu, Z. Y. Jiang and G. A. Ozin, Supercharged CO_2 Photothermal Catalytic Methanation: High Conversion, Rate, and Selectivity, *Angew. Chem., Int. Ed.*, 2023, **62**, e202218694.

2 Z. M. Yuan, X. H. Sun, H. Q. Wang, X. L. Zhao and Z. Y. Jiang, Applications of Ni-Based Catalysts in Photothermal CO_2 Hydrogenation Reaction, *Molecules*, 2024, **29**, 3882.

3 C. Zuo, Q. Su and X. Y. Yan, Research Progress of Co-Catalysts in Photocatalytic CO_2 Reduction: A Review of Developments, Opportunities, and Directions, *Processes*, 2023, **11**, 867.

4 Z. M. Yuan, X. L. Zhu and Z. Y. Jiang, Recent Advances of Constructing Metal/Semiconductor Catalysts Designing for Photocatalytic CO_2 Hydrogenation, *Molecules*, 2023, **28**, 5693.

5 C. Zuo, X. S. Tai, Z. Y. Jiang, M. F. Liu, J. H. Jiang, Q. Su and X. Y. Yan, S-Scheme 2D/2D Heterojunction of $ZnTiO_3$ Nanosheets/Bi_2WO_6 Nanosheets with Enhanced Photoelectrocatalytic Activity for Phenol Wastewater under Visible Light, *Molecules*, 2023, **28**, 3495.

6 L. K. Wang, T. T. Zhou, Z. Cao, *et al.*, Regulating the atomic ratio of Pt/Ru to enhance CO anti-poisoning of Pt based electrocatalysts toward methanol oxidation reaction, *Mol. Catal.*, 2024, **556**, 113927.

7 C. L. Xin, X. Jiao, Y. L. Yin, *et al.*, Enhanced CO_2 Adsorption Capacity and Hydrothermal Stability of HKUST-1 via Introduction of Siliceous Mesocellular Foams (MCFs), *Ind. Eng. Chem. Res.*, 2016, **556**, 113927.

8 Z. M. Yuan and Z. Y. Jiang, Applications of BiOX in the photocatalytic reactions, *Molecules*, 2023, **28**, 4400.

9 X. Q. Gao, L. L. Cao, Y. Chang, *et al.*, Improving the CO_2 Hydrogenation Activity of Photocatalysts via the Synergy between Surface Frustrated Lewis Pairs and the CuPt Alloy, *ACS Sustainable Chem. Eng.*, 2022, **11**, 5597–5607.

10 C. Zuo, X. Tang, H. Q. Wang and Q. Su, A Review of the Effect of Defect Modulation on the Photocatalytic Reduction Performance of Carbon Dioxide, *Molecules*, 2024, **29**, 2308.

11 Q. Su, C. Zuo, M. F. Liu and X. S. Tai, A Review on Cu_2O-Based Composites in Photocatalysis: Synthesis, Modification, and Applications, *Molecules*, 2023, **28**, 5576.

12 C. Zuo, Q. Su and Z. Y. Jiang, Advances in the Application of Bi-Based Compounds in Photocatalytic Reduction of CO_2, *Molecules*, 2023, **28**, 3982.

13 X. Tai, X. Yan and L. H. Wang, Synthesis, Structural Characterization, Hirschfeld Surface Analysis, Density Functional Theory, and Photocatalytic CO_2 Reduction Activity of a New Ca(II) Complex with a Bis-Schiff Base Ligand, *Molecules*, 2024, **29**, 1047.

14 X. L. Zhu, E. L. Zhou, X. S. Tai, H. B. Zong, J. J. Yi, Z. M. Yuan, X. L. Zhao, P. Huang, H. Xu and Z. Y. Jiang, g-C_3N_4 S-Scheme Homojunction through Van der Waals Interface Regulation by Intrinsic Polymerization Tailoring for Enhanced Photocatalytic H_2 Evolution and CO_2 Reduction, *Angew. Chem., Int. Ed.*, 2025, e202425439.

15 L. H. Wang, M. Azam, X. Yan and X. Tai, Synthesis, Structural Characterization, and Hirschfeld Surface Analysis of a New Cu(II) Complex and Its Role in Photocatalytic CO_2 Reduction, *Molecules*, 2024, **29**, 1957.

16 H. Lu, D. Fu, X. S. Tai, Z. L. Sun and X. K. Wang, Metal-Organic Frameworks/Covalent–Organic Frameworks-Based Materials in Organic/inorganic Pollutant Elimination and CO_2 Reduction Applications, *ChemNanoMat*, 2025, e202500244.

17 X. L. Zhao, X. Zhou, W. Y. Xing, *et al.*, Cu_3Pt_1 alloys confined by penta-coordinate Al^{3+} on Al_2O_3 realize CO oxidation at room temperature, *Mol. Catal.*, 2025, **570**, 114664.

18 S. Chu, P. F. Ou, P. Ghamari, *et al.*, Photoelectrochemical CO_2 reduction into syngas with the metal/oxide interface, *J. Am. Chem. Soc.*, 2018, **140**, 7869–7877.

19 Y. Ren, S. Han, C. Liu, Y. M. Feng, K. X. Li and M. J. Song, One-step Growth of Well Aligned K-doped ZnO Nanotapers Using a Facile Electrochemical Route: Photocatalyst Application, *Int. J. Electrochem. Sci.*, 2019, **14**, 6267–6275.

20 M. M. Xu, Y. Li, X. K. Wang, H. Y. Liu, Q. R. Liu, Y. F. Zhang, W. D. Fan, Q. G. Meng and D. F. Sun, Imidazole-Functionalized Zn-MOFs for One-Step C_2H_4 Purification from $C_2H_2/C_2H_4/C_2H_6$ Ternary Mixture, *Inorg. Chem.*, 2025, **64**, 813–817.

21 H. Y. Zhang and Q. Su, Recent Advances of Indium-Based Sulfides in Photocatalytic CO_2 Reductionl, *ACS Omega*, 2025, **10**, 8793–8815.

22 Z. M. Yuan, X. L. Zhu, Q. C. Gao and Z. Y. Jiang, Light Control-Induced Oxygen Vacancy Generation and In Situ Surface Heterojunction Reconstruction for Boosting CO_2 Reduction, *Molecules*, 2023, **28**, 4057.

23 J. A. L. Perini, L. D. M. Torquato, J. F. de Brito, *et al.*, Solar-driven CO_2 conversion to methane and methanol using different nanostructured Cu_2O-based catalysts modified with Au nanoparticles, *J. Energy Chem.*, 2024, **91**, 287–298.

24 R. Gusain, P. Kumar, O. P. Sharma, S. L. Jain and O. P. Khatri, Reduced Graphene Oxide-CuO Nanocomposites for Photocatalytic Conversion of CO_2 into Methanol under Visible Light Irradiation, *Appl. Catal., B*, 2016, **181**, 352–362.

25 S. K. Movahed, A. Najinasab, R. Nikbakht and M. Dabiri, Visible light assisted photocatalytic reduction of CO_2 tomethanol using Fe_3O_4@N-C/Cu_2O nanostructure photocatalyst, *J. Photochem. Photobiol., A*, 2020, **401**, 112763.

26 A. Al-Anazi, L. A. Al-Hajji, A. A. Ismail, A. M. El-Toni, A. Khan and Y. Huang, Anchored Li_2MnO_3 nanoparticles on ZnO nanosheets photocatalyst for effective CO_2 reduction to CH_3OH upon visible illumination, *Mater. Sci. Semicond. Process.*, 2025, **196**, 109654.

27 M. B. Getahun, S. Y. Ejeta, T. Imae and J. P. Chu, Effect of a three-dimensional nanotube array substrate on photocatalytic conversion performance of CO_2 gas to methanol by amine-loaded CuO/ZnO catalysts, *J. Colloid Interface Sci.*, 2024, **674**, 118–127.

28 S. K. Sahoo, P. Athira, K. Ray and D. Pandey, Addition of CuO to form CuO/TiO_2 and CuO/ZnO heterojunctions for photocatalytic CO_2 conversion to methanol, *Chem. Phys. Lett.*, 2024, **856**, 141678.

29 F. Li, L. Zhang, J. C. Tong, Y. L. Liu, S. G. Xu, Y. Cao and S. K. Cao, Photocatalytic CO_2 conversion to methanol by Cu_2O/graphene/TNA heterostructure catalyst in a visible-light-driven dual-chamber reactor, *Nano Energy*, 2016, **27**, 320–329.

30 X. J. Luo, L. Qiao, S. T. Zhang, *et al.*, S-vacancy-assisted dual-sites on $NiCo_2S_4$ for photo conversion of CO_2 to olefiant gas, *Appl. Surf. Sci.*, 2022, **601**, 1–9.

31 M. Imran, W. Ashraf, A. K. Hafiz and M. Khanuja, Synthesis and Performance Analysis of Photocatalytic Activity of $ZnIn_2S_4$ Microspheres Synthesized Using a Low-Temperature Method, *ACS Omega*, 2022, **7**, 22987–22996.

32 R. M. Mohamed, I. A. Mkhalid, M. Alhaddad, *et al.*, Facile fabrication of Pt-doped mesoporous ZnS as high efficiency for photocatalytic CO_2 conversion, *J. Inorg. Organomet. Polym.*, 2021, **31**, 4637–4647.

33 X. Wang, W. L. Zeng and C. L. Xin, The development of activated carbon from corncob for CO_2 capture, *RSC Adv.*, 2022, **12**, 33069–33078.

34 P. M. Gawal and A. K. Golder, Vegetal route for synthesis of CQDs/CdS nanocomposites for photocatalytic reduction of CO to methanol under visible light, *Colloids Surf., A*, 2024, **683**, 133068.

35 M. Cheng, S. X. Bai, Y. Z. Xia, X. Zhu, R. Chen and Q. Liao, Highly efficient photocatalytic conversion of gas phase CO by TiO nanotube array sensitized with CdS/ZnS quantum dots under visible light, *Int. J. Hydrogen Energy*, 2021, **46**, 31634–31646.

36 W. Q. Luo, Y. H. Yi, L. Duan, *et al.*, $Zn_{0.5}Cd_{0.5}S$ photocatalysts with loaded Cu^{2+} and Ni^{2+} dual active sites for promoted syngas production, *J. Mater. Chem. A*, 2025, **13**, 20641–20649.

37 L. P. Sun, W. T. Wu, R. P. Wei, *et al.*, Construction of an S-scheme Bi_2S_3/$CdIn_2S_4$ heterojunction for the photocatalytic generation of methyl formate, *New J. Chem.*, 2023, **47**, 19235–19242.

38 M. Baniamer, A. Aroujalian and S. Sharifnia, A novel PEBAX-1657/PES-(BiFeO@ZnS) photocatalytic membrane for integrated hybrid systems coupling CO separation and photoreduction, *J. Environ. Chem. Eng.*, 2021, **9**, 106529.

39 N. M. Yusop, O. P. Ching, S. Sufian and M. M. Zain, Enhanced Effect of Metal Sulfide Doping (MgS-TiO_2) Nanostructure Catalyst on Photocatalytic Reduction of CO_2 to Methanol, *Sustainability*, 2023, **15**, 10415.

40 J. M. Zhang, X. C. Xu, X. Guo, N. Liu, X. F. Ma, H. W. Ren, H. Xiao, M. Zhao, B. L. Lv, J. X. Tang, T. J. Hu and J. F. Jia, PdMoW trimetallene facilitates the electrooxidation of ethanol in alkaline electrolyte with high efficiency and C2 selectivity, *J. Colloid Interface Sci.*, 2026, **702**, 1389172.

41 S. F. Zhang, X. H. Yin and Y. A. Zheng, Enhanced photocatalytic reduction of CO_2 to methanol by ZnO nanoparticles deposited on ZnSe nanosheet, *Chem. Phys. Lett.*, 2018, **693**, 170–175.

42 A. Li, T. Wang, C. C. Li, *et al.*, Adjusting the reduction potential of electrons by quantum confinement for selective photoreduction of CO_2 to methanol, *Angew. Chem., Int. Ed.*, 2019, **58**, 3804–3808.

43 A. Ali and W. C. Oh, Preparation of nanowire like WSe_2-graphene nanocomposite for photocatalytic reduction of CO_2 into CH_3OH with the presence of sacrificial agents, *Sci. Rep.*, 2017, **7**, 3282390.

44 X. L. Zhao, Q. H. Zhang, J. F. Yang and X. Y. Wu, Realizing the high loading amount of active Cu on Al_2O_3 to boost its CO catalytic oxidation, *J. Colloid Interface Sci.*, 2024, **673**, 669–678.

45 L. H. Wang and X. S. Tai, Synthesis, structural characterization, Hirschfeld surface analysis and photocatalytic CO_2 reduction activity of a new dinuclear Gd (III) complex with 6-phenylpyridine-2-carboxylic acid and 1,10-phenanthroline ligands, *Molecules*, 2023, **28**, 7595.

46 X. Wang, W. L. Zeng, H. Y. Zhang, D. Li, H. J. Tian, X. D. Hu, Q. Wu, C. L. Xin, X. Y. Cao and W. J. Liu, The dynamic CO_2 adsorption of polyethylene polyamine-loaded MCM-41 before and after methoxypolyethylene glycol codispersion, *RSC Adv.*, 2019, **9**, 27050–27059.

47 X. Wang, W. L. Zeng, W. J. Liu, X. Y. Cao, C. H. Hou, D. Qi and Y. X. Lü, CO_2 adsorption of lignite chars after one-step KOH activation, *New J. Chem.*, 2020, **44**, 13755–13763.

48 C. L. Xin, Y. Ren, Z. F. Zhang, L. L. Liu, X. Wang and J. M. Yang, Enhancement of Hydrothermal Stability and CO_2 Adsorption of Mg-MOF-74/MCF Composites, *ACS Omega*, 2021, **6**, 7739–7745.

49 X. Wang, W. L. Zeng, C. L. Xin, X. J. Kong, X. D. Hu and Q. J. Guo, The development of activated carbon from corncob for CO_2 capture, *RSC Adv.*, 2022, **12**, 33069–33078.

50 X. Wang, W. L. Zeng, X. J. Kong, C. L. Xin, Y. N. Dong, X. D. Hu and Q. J. Guo, Development of Low-Cost Porous Carbons through Alkali Activation of Crop Waste for CO_2 Capture, *ACS Omega*, 2022, **7**, 46992–47001.

51 S. H. Cao, J. L. Fan, W. Sun, F. H. Li, K. X. Li, X. S. Tai and X. J. Peng, A novel Mn–Cu bimetallic complex for enhanced chemodynamic therapy with simultaneous glutathione depletion, *Chem. Commun.*, 2019, **55**, 12956–12959.

52 S. H. Cao, F. H. Li, Q. Xu, M. Yao, *et al.*, Synthesis, crystal structure of a novel tetranuclear Cu (ii) complex and its application in GSH-triggered generation of reactive oxygen species for chemodynamic therapy, *J. Saudi Chem. Soc.*, 2021, **25**, 101372.

53 X. K. Niu, M. M. Li, T. T. Liu, Y. D. Yang, J. T. Lu and X. M. Zhang, Three-dimensional DNA Walker-mediated polarity switching biosensor based on the heterostructure of COFs and CuO nanocube for the sensitive photoelectrochemical detection of silver, *Sens. Actuators, B*, 2025, **426**, 137019.

54 L. Wang, P. C. Liu, M. Z. Wang, T. R. Wei, J. Lu, X. L. Zhao, Z. Y. Jiang, Z. M. Yuan, X. J. Liu and J. He, Modulating d-d orbitals coupling in PtPdCu medium-entropy alloy aerogels to boost pH-general methanol electrooxidation performance, *Chin. Chem. Lett.*, 2025, **36**, 110532.

55 Z. Guo, J. Zhou, L. Zhu and Z. Sun, MXene: a promising photocatalyst for water splitting, *J. Mater. Chem. A*, 2016, **4**, 11446–11452.

56 M. Asadi, C. Liu, A. V. Addepalli, P. Abbasi, P. Yasaei, P. Phillips, A. Behranginia, J. M. Cerrato, R. Haasch, P. Zapol, B. Kumar, R. F. Klie, J. Abiade, L. A. Curtiss and A. Salehi-Khojin, Nanostructured transition metal dichalcogenide electrocatalysts for CO_2 reduction in ionic liquid, *Science*, 2016, **353**, 467–470.

57 M. F. Kuehnel, C. D. Sahm, G. Neri, J. R. Lee, K. L. Orchard, A. J. Cowan and E. Reisner, ZnSe quantum dots modified with a Ni (cyclam) catalyst for efficient visible-light driven CO_2 reduction in water, *Chem. Sci.*, 2018, **9**, 2501–2509.

58 C. L. Xin, X. Jiao, Y. L. Yin, *et al.*, Enhanced CO_2 Adsorption Capacity and Hydrothermal Stability of HKUST-1 via Introduction of Siliceous Mesocellular Foams (MCFs), *Ind. Eng. Chem. Res.*, 2016, **55**, 7950–7957.

59 C. Yan, G. Chen, Y. Q. Zhang, D. H. Chen, J. Pei and Z. Z. Qiu, $CuSe_{1-x}S_x$ nanosheets with an ordered superstructure as anode materials for lithium-ion batteries, *New J. Chem.*, 2016, **40**, 6588–6592.

60 D. Chen, G. Chen, R. Jin and H. Xu, Self-decorated $Cu_{2-x}Se$ nanosheets as anode materials for Li ion batteries and electrochemical hydrogen storage, *CrystEngComm*, 2014, **16**, 2810–2817.

61 K. L. Wang, M. Z. Wang, Q. Z. Lei, T. T. Zhou, X. J. Liu, Z. Cao, Z. Y. Jiang and J. He, Strain effect of PtCu alloy aerogel nanocatalysts on the oxygen reduction reaction enhancement, *Mol. Catal.*, 2025, **580**, 115121.

62 D. X. Yang, Q. G. Zhu, C. J. Chen, H. Z. Liu, Z. M. Liu, Z. J. Zhao, X. Y. Zhang, S. J. Liu and B. X. Han, Selective electroreduction of carbon dioxide to methanol on copper selenide nanocatalysts, *Nat. Commun.*, 2019, **10**, 667.

63 D. X. Yang, Q. G. Zhu, X. F. Sun, C. J. Chen, W. W. Guo, G. Y. Yang and B. X. Han, Electrosynthesis of a defective indium selenide with 3D structure on a substrate for tunable CO_2 electroreduction to syngas, *Angew. Chem., Int. Ed.*, 2019, **59**, 2354–2359.

64 K. Sonowal, N. Nandal, P. Basyach, L. Kalita, S. L. Jain and L. Saikia, Photocatalytic reduction of CO_2 to methanol using Zr(IV)-based MOF composite with g-C_3N_4 quantum dots under visible light irradiation, *J. CO2 Util.*, 2022, **57**, 101905.

65 B. Y. Rameshwar, M. S. Ramyashree, T. Lakshmi, *et al.*, Waste-derived Ag@Cu-MOF with semiconductor functionalized nano-hybrid heterostructures for photocatalytic CO_2 conversion to methanol fuel, *J. Environ. Manage.*, 2025, **391**, 126508.

66 L. Y. Zhang, G. H. Zhou, G. R. Chen, *et al.*, Bimetallic NiCu catalyst derived from spent MOF adsorbent for efficient photocatalytic CO_2 reduction, *Chem. Eng. J.*, 2024, **497**, 154701.

67 Q. Y. Zhang, Y. J. Chen, X. Y. Yu, Y. J. Yin, Y. X. Ru and G. H. Tian, In situ construction of Schottky junctions on MOF-derived defective TiO_2 oval nanocages for enhanced photocatalytic CO_2 reduction, *J. Alloys Compd.*, 2024, **983**, 173735.

68 Q. Zhao, S. Q. Yang, S. Zhang, *et al.*, Single MOF Based on Asymmetric Intramolecular Electron Compartments Enables Highly Efficient Photocatalytic CO_2 Overall Reaction to Methanol, *Angew. Chem., Int. Ed.*, 2025, **65**, e20298.

69 Y. Wang, J. Z. Zhao, Y. M. Liu, *et al.*, Synergy between plasmonic and sites on gold nanoparticle-modified bismuth-rich bismuth oxybromide nanotubes for the efficient photocatalytic CAC coupling synthesis of ethane, *J. Colloid Interface Sci.*, 2022, **616**, 649–658.

70 N. N. Zhang, J. H. Ji, X. R. Pan and M. Y. Xing, Research progress of graphene-based nanomaterials for the environmental remediation, *Chin. Chem. Lett.*, 2020, **31**, 1462–1473.

71 X. R. Pan, F. Y. Kong and M. Y. Xing, Spatial separation of photo-generated carriers in g-C_3N_4/MnO_2/Pt with enhanced H_2 evolution and organic pollutant control, *Res. Chem. Intermed.*, 2022, **48**, 2837–2855.

72 S. Kreft, R. Schoch and J. Schneidewind, Improving selectivity and activity of CO_2 reduction photocatalysts with oxygen, *Chem*, 2019, **5**, 1818–1833.

73 Z. Zhang, B. Wang, H. B. Zhao, *et al.*, Self-assembled lead-free double perovskite-MXene heterostructure with efficient charge separation for photocatalytic CO_2 reduction, *Appl. Catal., B*, 2022, **312**, 121358.

74 Y. N. Zheng, X. H. Yin, Y. Jiang, *et al.*, Nano Ag-decorated MoS_2 nanosheets from 1T to 2H phase conversion for photocatalytically reducing CO_2 to methanol, *Energy Technol.*, 2019, **7**, 1900582.

75 P. K. Prajapati, H. Singh, R. Yadav, *et al.*, Core-shell Ni/NiO grafted cobalt (II) complex: an efficient inorganic nanocomposite for photocatalytic reduction of CO_2 under visible light irradiation, *Appl. Surf. Sci.*, 2019, **467**, 370–381.

76 F. Iqbal, A. Mumtaz, S. Shahabuddin, *et al.*, Photocatalytic reduction of CO_2 to methanol over $ZnFe_2O_4$/TiO_2 (p–n) heterojunctions under visible light irradiation, *J. Chem. Technol. Biotechnol.*, 2020, **95**, 2208–2221.

77 T. P. Yendrapati-Taraka, A. Gautam, S. L. Jain, *et al.*, Controlled addition of Cu/Zn in hierarchical CuO/ZnO p–n heterojunction photocatalyst for high photoreduction of CO_2 to MeOH, *J. CO2 Util.*, 2019, **31**, 207–214.

78 H. L. Zhao, F. P. Pan and Y. Li, A review on the effects of TiO_2 surface point defects on CO_2 photoreduction with H_2O, *J. Inorg. Mater.*, 2017, **3**, 17–32.

79 C. Z. Zhu, X. Q. Wei, W. Q. Li, *et al.*, Crystal-plane effects of CeO_2 {110} and CeO_2 {100} on photocatalytic CO_2 reduction: synergistic interactions of oxygen defects and hydroxyl groups, *ACS Sustain. Chem. Eng.*, 2020, **8**, 14397–14406.

80 S. H. Cao, F. H. Li, Q. Xu, *et al.*, Synthesis, crystal structure of a novel tetranuclear Cu (ii) complex and its application in GSH-triggered generation of reactive oxygen species for chemodynamic therapy, *J. Saudi Chem. Soc.*, 2021, **25**, 101372.

81 T. T. Zhou, Z. Cao, X. S. Tai, *et al.*, Hierarchical $Co(OH)_2$ Dendrite Enriched with Oxygen Vacancies for Promoted Electrocatalytic Oxygen Evolution Reaction, *Polymers*, 2022, **14**, 1510.

82 C. Han, J. Li, Z. Ma, *et al.*, Black phosphorus quantum dot/g-C_3N_4 composites for enhanced CO_2 photoreduction to CO, *Sci. China Mater.*, 2018, **61**, 1159–1166.

83 L. M. Xue, F. H. Zhang, H. J. Fan, *et al.*, Preparation of C doped TiO_2 photocatalysts and their photocatalytic reduction of carbon dioxide, *Adv. Mater. Res.*, 2011, **183–185**, 1842–1846.

84 B. Michalkiewicz, J. Majewska, G. Ka, *et al.*, Reduction of CO_2 by adsorption and reaction on surface of TiO_2-nitrogen modified photocatalyst, *J. CO2 Util.*, 2014, **5**, 47–52.

85 O. Ola and M. M. Maroto-Valer, Transition metal oxide based TiO_2 nanoparticles for visible light induced CO_2 photoreduction, *Appl. Catal., A*, 2015, **502**, 114–121.

86 M. Tahir and N. S. Amin, Indium-doped TiO_2 nanoparticles for photocatalytic CO_2 reduction with H_2O vapors to CH_4, *Appl. Catal., B*, 2015, **162**, 98–109.

87 D. Kong, J. Z. Y. Tan, F. Yang, *et al.*, Electrodeposited Ag nanoparticles on TiO_2 nanorods for enhanced UV visible light photoreduction CO_2 to CH_4, *Appl. Surf. Sci.*, 2013, **277**, 105–110.

88 Q. Du, J. Liu, C. Chung, *et al.*, Photocatalytic reduction of CO_2 on $FeTiO_3/TiO_2$ photocatalyst, *Catal. Commun.*, 2012, **19**, 85–89.

89 B. A. Ahmad, S. Fatemi and Z. Salehi, Synthesis of nanocomposite CdS/TiO_2 and investigation of its photocatalytic activity for CO_2 reduction to CO and CH_4 under visible light irradiation, *J. CO_2 Util.*, 2014, **7**, 23–29.

90 Q. Wu, Q. P. Gao, B. Shan, *et al.*, Recent advances in self-supported transition-metal-based electrocatalysts for seawater oxidation, *Acta Phys.-Chim. Sin.*, 2023, **39**, 2303012.

91 Q. Wu and J. Li, One-Step Preparation of Cobalt-Nanoparticle-Embedded Carbon for Effective Water Oxidation Electrocatalysis, *ChemElectroChem*, 2019, **6**, 1996–1999.

92 X. Y. Wang, M. Q. Geng, S. J. Sun, *et al.*, Recent advances of bifunctional electrocatalysts and electrolyzers for overall seawater splitting, *J. Mater. Chem. A*, 2024, **12**, 634–656.

93 Q. Wu, Q. P. Gao, X. P. Wang, *et al.*, Boosting electrocatalytic performance *via* electronic structure regulation for acidic oxygen evolution, *iScience.*, 2024, **27**, 108738.

94 Y. D. Yang, X. K. Niu, B. Q. Duan, J. T. Lu and X. M. Zhang, Dual-modal biosensor for mercuric ion detection based on $Cu_2O@Cu_2S$/D-TA COF heterojunction with excellent catalase-like, electrochemical and photoelectrochemical properties with excellent catalase-like, electrochemical and photoelectrochemical properties, *Biosens. Bioelectron.*, 2024, **262**, 116568.

95 Z. M. Yuan, H. H. Miao, Z. Y. Jiang, X. L. Zhao, S. K. Shi and X. L. Zhu, Oxygen vacancy activated inlaid Fe active sites in WO_3 for sustainable and efficient photo-Fenton oxidation in a wide pH range, *Mol. Catal.*, 2025, **577**, 114962.

96 H. M. Guo, L. Liu and Q. Wu, Cu_3N nanowire array as a high-efficiency and durable electrocatalyst for oxygen evolution reaction, *Dalton Trans.*, 2019, **48**, 5131–5134.

97 A. H. Behroozi and R. Xu, Photocatalytic CO_2 reduction: Photocatalysts, membrane reactors, and hybrid processes, *Chem Catal.*, 2023, **3**, 100550.

98 J. C. S. Wu, T. H. Wu, T. C. Chu, H. J. Huang and D. P. Tsai, Application of optical-fiber photoreactor for CO_2 photocatalytic reduction, *Top. Catal.*, 2008, **47**, 131–136.

99 T. V. Nguyen and J. C. S. Wu, Photoreduction of CO_2 in an optical-fiber photoreactor: effects of metals addition and catalyst carrier, *Appl. Catal., A*, 2008, **335**, 112–120.

100 O. Ola, M. M. Valer, D. Liu, S. Mackintosh, C. W. Lee and J. C. S. Wu, Performance comparison of CO_2 conversion in slurry and monolith photoreactors using Pd and Rh-TiO_2 catalyst under ultraviolet irradiation, *Appl. Catal., B*, 2012, **126**, 172–179.

101 Z. Zhang, W. A. Anderson and M. Moo-Young, Experimental analysis of a corrugated plate photocatalytic reactor, *Chem. Eng. J.*, 2004, **99**, 145–152.

102 M. Mehrpooya and F. Bayatlar, Photocatalytic Reactors for CO_2 Reduction: Review on Simulation Studies, *Arch. Comput. Methods Eng.*, 2026, **33**, 2605–2657.

103 L. K. Pan, M. G. Zhang, H. Mei, *et al.*, 3D bionic reactor optimizes photon and mass transfer by expanding reaction space to enhance photocatalytic CO_2 reduction, *Sep. Purif. Technol.*, 2022, **301**, 121974.

104 F. Galli, M. Compagnoni, D. Vitali, C. Pirola, C. L. Bianchi, A. Villa, L. Prati and I. Rossetti, CO_2 Photoreduction at High Pressure to Both Gas and Liquid Products over Titanium Dioxide, *Appl. Catal., B*, 2017, **200**, 386–391.

105 E. George, A. Essa, B. Yasmine, D. Matyas, E. Salvador and H. Klaus, Simultaneous photocatalytic CO_2 reduction and C-C coupling of benzyl alcohol under high pressure and supercritical conditions, *Chem. Eng. J.*, 2025, **505**, 158356.

106 R. Wang, M. J. Zhang, S. L. Zhang, J. Z. Zheng, Y. Q. Zeng, Y. Yang, J. Ding, X. Wu and Q. Zhong, Self-Supporting Triphase Photocatalytic CO_2 Reduction to CH_3OH on Controllable Core-Shell Structure with Tunable Interfacial Wettability, *ACS Nano*, 2023, **17**, 24363–24373.

107 Z. Lu, Y. F. Xu, Z. S. Zhang, J. C. Sun, X. Ding, W. Sun, W. G. Tu, Y. Zhou, Y. F. Yao, G. A. Ozin, L. Wang and

Z. G. Zou, Wettability Engineering of Solar Methanol Synthesis, *J. Am. Chem. Soc.*, 2023, **145**, 26052–26060.

108 B. Shang, F. Y. Zhao, S. Suo, Y. Z. Gao, *et al.*, Tailoring Interfaces for Enhanced Methanol Production from Photoelectrochemical CO_2 Reduction, *J. Am. Chem. Soc.*, 2024, **146**, 2267–2274.

109 F. R. Pomilla, A. Brunetti, G. Marci, E. L. G. Lopez, E. Fontananova, L. Palmisano and G. Barbieri, CO_2 to liquid fuels: photocatalytic conversion in a continuous membrane reactor, *ACS Sustainable Chem. Eng.*, 2018, **6**, 8743–8753.

110 F. Rechberger and M. Niederberger, Translucent nanoparticle-based aerogel monoliths as 3-dimensional photocatalysts for the selective photoreduction of CO_2 to methanol in a continuous flow reactor, *Mater. Horiz.*, 2017, **4**, 1115–1121.

111 M. M. Mirzaei, V. M. Avargani, S. A. A. Mirjalily and S. A. A. Oloomi, Synergistic photothermal CO -to-methanol conversion using concentrated solar energy: CFD modeling of a novel packed monolith-fiber cavity reactor, *Fuel*, 2026, **416**, 138532.

112 K. Vinodgopal, S. Hotchandani and P. V. Kamat, Electrochemically assisted photocatalysis: titania particulate film electrodes for photocatalytic degradation of 4-chlorophenol, *J. Phys. Chem.*, 1993, **97**, 9040–9044.

113 J. Yang, C. C. Chen and H. W. Ji, Mechanism of TiO_2-Assisted Photocatalytic Degradation of Dyes under Visible Irradiation: Photoelectrocatalytic Study by TiO_2-Film Electrodes, *J. Phys. Chem. B*, 2005, **109**, 21900–21907.

114 Y. L. Xu, D. J. Zhong and J. P. Jia, Electrochemical-assisted photodegradation of Allura Red and textile effluent using a half exposed rotating TiO_2/Ti disc electrode, *J. Environ. Sci. Health, Part A*, 2008, **43**, 503–510.

115 Z. Zhang, W. A. Anderson and M. Moo-Young, Rigorous modeling of UV absorption by TiO_2 films in a photocatalytic reactor, *AIChE J.*, 2000, **46**, 1461–1470.

116 Z. X. Lin, J. Y. Zhang, Z. Xiong and Y. C. Zhao, Enhanced photocatalytic CO_2 reduction in a twin reactor by separating triphase CO_2 reduction and water oxidation reactions, *Chem. Eng. J.*, 2025, **507**, 160734.

117 F. N. A. R. Lim, F. Marpani, V. E. A. Dilol, *et al.*, A Review on the Design and Performance of Enzyme-Aided Catalysis of Carbon Dioxide in Membrane, Electrochemical Cell and Photocatalytic Reactors, *Membranes*, 2021, **12**, 28.

118 S. H. Chen, R. Ding, B. Y. Li, J. T. Lu and X. M. Zhang, A robust aerogel incorporated with phthalocyanine-based porous organic polymers for highly efficient gold extraction, *Sep. Purif. Technol.*, 2025, **354**, 129451.

119 H. Guo, W. X. Chen, X. Q. Qiao, *et al.*, Skillful promotion of charge separation *via* defect-mediated built-in electric field and LSPR effect for enhanced photocatalytic activity, *Nano Energy*, 2025, **135**, 110672.

120 W. L. Wang, Q. L. Liu, L. Zhang, Y. C. Dong and J. Du, RetroSynX: A retrosynthetic analysis framework using hybrid reaction templates and group contribution-based thermodynamic models, *Chem. Eng. Sci.*, 2021, **248**, 117208.

121 X. Li, P. Y. Gao, Y. Y. Lai, *et al.*, Symmetry-breaking design of an organic iron complex catholyte for a long cyclability aqueous organic redox flow battery, *Nat. Energy*, 2021, **6**, 873–881.

122 Y. Q. Ren, S. N. Lan, Y. H. Zhu, R. X. Peng, H. B. He, Y. T. Si, K. Huang and N. X. Li, Concentrated Solar-Driven Catalytic CO_2 Reduction: From Fundamental Research to Practical Applications, *ChemSusChem*, 2025, **18**, e202402485.

123 L. Xu, Y. Y. Ren, Y. W. Fu, M. C. Liu, F. F. Zhu, M. Cheng, J. C. Zhou, W. S. Chen, K. Wang, N. Wang and N. X. Li, Strong photo-thermal coupling effect boosts CO reduction into CH in a concentrated solar reactor, *Chem. Eng. J.*, 2023, **468**, 143831.

124 Q. Zhang, Q. Zhang, H. Wang and Y. Li, A high efficiency microreactor with Pt/ZnO nanorod arrays on the inner wall for photodegradation of phenol, *J. Hazard. Mater.*, 2013, **254**, 318–324.

125 G. Yu and N. Wang, Gas-liquid-solid interface enhanced photocatalytic reaction in a microfluidic reactor for water treatment, *Appl. Catal., A*, 2020, **591**, 117410.

126 A. Yusuf and G. Palmisano, Three-dimensional CFD modelling of a photocatalytic parallel-channel microreactor, *Chem. Eng. Sci.*, 2021, **229**, 116051.

127 L. Suhadolnik, M. Krivec, K. Zagar, G. Drazic and M. Ceh, A TiO_2-nanotubes -based coil-type microreactor for highly efficient photo-electrocatalytic degradation of organic compounds, *J. Ind. Eng. Chem.*, 2017, **47**, 384–390.

128 O. Ola and M. M. Maroto-Valer, Synthesis, characterization and visible light photocatalytic activity of metal based TiO_2 monoliths for CO_2 reduction, *Chem. Eng. J.*, 2016, **283**, 1244–1253.

129 M. Tahir, V_2AlC MAX-mediated 2D/0D $ZnCo_2O_4$ NS/TiO_2 Z-scheme heterojunctions with enhanced photocatalytic CO_2 bireforming *via* synergistic charge transfer in a monolith and flow reactor, *Fuel*, 2025, **404**, 136206.

130 M. Tahir and N. Kumar, Highly stable 2D/2D $ZnCo_2O_4$ NSL/pg-C_3N_4 composite with defective sites for enhancing selective photocatalytic CO_2 reduction in a batch/continuous flow reactor, *Energy Convers. Manage.: X*, 2025, **28**, 101311.

131 S. Nabil, E. A. Shalaby, M. F. Elkady, Y. Matsushita and A. H. El-Shazly, Optimizing the Performance of the Meso-Scale Continuous-Flow Photoreactor for Efficient Photocatalytic CO_2 Reduction with Water Over Pt/TiO_2/RGO Composites, *Catal. Lett.*, 2022, **152**, 3243–3258.

132 X. Cheng, R. Chen, X. Zhu, Q. Liao, L. An, D. D. Ye, X. F. He, S. Z. Li and L. Li, An optofluidic planar microreactor for photocatalytic reduction of CO_2 in alkaline environment, *Energy*, 2017, **120**, 276–282.

133 A. J. Li, F. Liang, X. Y. Li, Z. B. Wang, P. K. Liu and L. Y. Zhu, Experimental study of dynamic characteristics of solid holdup fluctuations in a gas-solid cyclone reactor, *Chem. Eng. Res. Des.*, 2024, **203**, 67–477.

134 J. Albo, M. I. Qadir, M. Samperi, J. A. Fernandes, I. D. Pedro and J. Dupon, Use of an optofluidic microreactor and Cu nanoparticles synthesized in ionic liquid and embedded

in TiO_2 for an efficient photoreduction of CO_2 to methanol, *Chem. Eng. J.*, 2021, **404**, 126643.

135 W. Morawski, K. Ćmielewska, E. Ekiert, *et al.*, Effective green ammonia synthesis from gaseous nitrogen and CO_2 saturated-water vapour utilizing a novel photocatalytic reactor, *Chem. Eng. J.*, 2022, **446**, 137030.

136 F. Xie, R. Chen, X. Zhu, *et al.*, CO_2 utilization: direct power generation by a coupled system that integrates photocatalytic reduction of CO_2 with photocatalytic fuel cell, *J. CO2 Util.*, 2019, **32**, 31–36.

137 K. K. Sakimoto, A. B. Wong and P. Yang, Self-photosensitization of nonphotosynthetic bacteria for solar-to-chemical production, *Science*, 2016, **351**, 74–77.

138 H. Zhang, H. Liu, Z. Tian, *et al.*, Bacteria photosensitized by intracellular gold nanoclusters for solar fuel production, *Nat. Nanotechnol.*, 2018, **13**, 900–905.